Inorganic Chemistry

Article

pubs.acs.org/IC

Di-, Tri-, and Tetranuclear Nickel(II) Complexes with Oximato Bridges: Magnetism and Catecholase-like Activity of Two Tetranuclear Complexes Possessing Rhombic Topology

Lakshmi Kanta Das,[†] Apurba Biswas,[†] Jared S. Kinyon,[‡] Naresh S. Dalal,[‡,*] Haidong Zhou,[§] and Ashutosh Ghosh[†,*]

[†]Department of Chemistry, University College of Science, University of Calcutta, 92 A.P.C. Road, Kolkata 700 009, India

[‡]Department of Chemistry & Biochemistry, Florida State University, Tallahassee, Florida 32306-4390, United States

[§]National High Magnetic Field Laboratory, Tallahassee, Florida 32310-3706, United States

Supporting Information

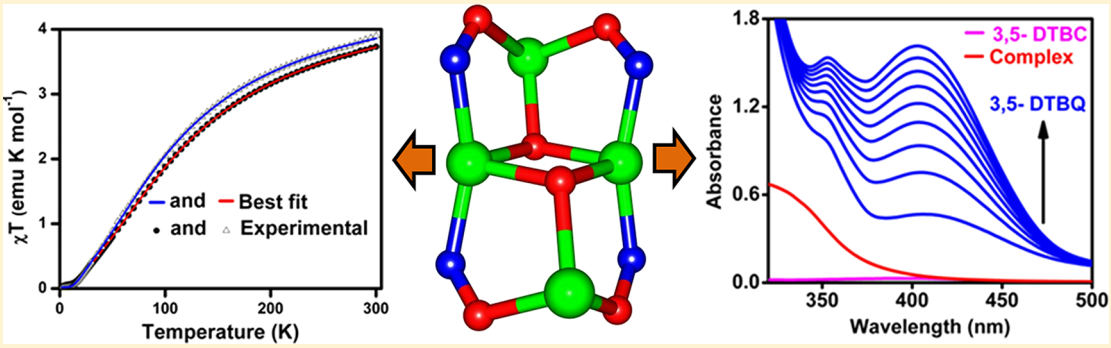

ABSTRACT: Oxime-based tridentate Schiff base ligands 3-[2-(diethylamino)ethylimino]butan-2-one oxime (HL^1) and 3-[3-(dimethylamino)propylimino]butan-2-one oxime (HL^2) produced the dinuclear complex $[Ni_2L^1_2](ClO_4)_2$ (**1**) and trinuclear complex $[Ni_3(HL^2)_3(\mu_3\text{-}O)](ClO_4)_4\cdot CH_3CN$ (**2**), respectively, upon reaction with $Ni(ClO_4)_2\cdot 6H_2O$. However, in a slightly alkaline medium, both of the ligands underwent hydrolysis and resulted in tetranuclear complexes $[\{Ni(deen)(H_2O)\}_2(\mu_3\text{-}OH)_2\{Ni_2(moda)_4\}](ClO_4)_2\cdot 2CH_3CN$ (**3**) and $[\{Ni(dmpn)(CH_3CN)_2\}_2(\mu_3\text{-}OH)_2\{Ni_2(moda)_4\}](ClO_4)_2\cdot CH_3CN$ (**4**), where deen = 2-(diethylamino)ethylamine, dmpn = 3-(dimethylamino)-1-propylamine, and modaH = diacetyl monoxime. All four complexes have been structurally characterized. Complex **1** is a centrosymmetric dimer where the square planar nickel(II) atoms are joined solely by the oximato bridges. In complex **2**, three square planar nickel atoms form a triangular core through a central oxido (μ_3-O) and peripheral oximato bridges. Tetranuclear complexes **3** and **4** consist of four distorted octahedral nickel(II) ions held together in a rhombic chair arrangement by two central μ_3-OH and four peripheral oximato bridges. Magnetic susceptibility measurements indicated that dinuclear **1** and trinuclear **2** exhibited diamagnetic behavior, while tetranuclear complexes **3** and **4** were found to have dominant antiferromagnetic intramolecular coupling with concomitant ferromagnetic interactions. Despite its singlet ground state, both **3** and **4** serve as useful examples of Kahn's model for competing spin interactions. High-frequency EPR studies were also attempted, but no signal was detected, likely due to the large energy gap between the ground and first excited state. Complexes **3** and **4** exhibited excellent catecholase-like activity in the aerial oxidation of 3,5-di-*tert*-butylcatechol to the corresponding *o*-quinone, whereas **1** and **2** did not show such catalytic activity. Kinetic data analyses of this oxidation reaction in acetonitrile revealed that the catalytic activity of **3** (k_{cat} = 278.4 h^{-1}) was slightly lower than that of **4** (k_{cat} = 300.0 h^{-1}). X-band EPR spectroscopy indicated that the reaction proceeded through the formation of iminoxyl-type radicals.

INTRODUCTION

The development of polynuclear transition-metal complexes are of current interest due to their wide range of applications in various fields such as catalysis, adsorption, storage, magnetism, molecular recognition, fluorescence, nonlinear optics, and sensors.[1] Molecular materials synthesized to study one particular property can be made multifunctional by judiciously selecting the metal ions and ligands. For example, a magnetic material can be used as a catalyst if nuclearity, flexibility, metal coordination sphere, and ligand substitution of the framework can be adjusted over a wide range for a variety of catalytic reactions.[2,3]

The coordination compounds are invaluable in the study of interesting magnetic phenomena like spin frustration, spin canting, spin glass transitions, and single molecule magnetism.[4] For this purpose, it is necessary to synthesize polynuclear complexes of a targeted topology and predefined number of

Received: April 24, 2013

   dx.doi.org/10.1021/ic401020m | Inorg. Chem. XXXX, XXX, XXX–XXX

metal atoms. Among the aforementioned properties, spin frustration[5] is an important topic stemming from the topological arrangement of spins. It has been well established in complexes where the spins are arranged in a triangular geometry[6] such as the widely employed $M_3(\mu_3\text{-}O)$ clusters, with M being Fe^{III}, Fe^{II}, Co^{II}, Ni^{II}, Cu^{II}, or Cr^{III}. This phenomenon has also been studied for tetranuclear Mn^{III}, Fe^{III}, or Ni^{II} complexes such as the M_4O_2 core (where M = Ni(II), Fe(III), and Mn(III)) possessing either a butterfly or rhombic topology.[7−10] Oxime ligands exhibit a noteworthy ability to bridge metal ions[9−11] and are known to produce such tri- or tetranuclear complexes with spin frustration.[9,10] Recently, we have reported a hexanuclear Cu^{II} complex with a triangular Cu_3O core synthesized through the use of a tridentate oxime based Schiff base ligand.[12] In the present work, our aim is to characterize oxime based multinuclear Ni(II) complexes in order to study their magnetic behavior and catecholase activity.

Catecholase-like activity of some model coordination complexes has been a topic of recent interest for the development of new bioinspired catalysts.[13] Catechol oxidase is a copper-containing type-III active-site protein that catalyzes the oxidation reaction of a wide range of *o*-diphenols (catechols) to corresponding *o*-quinones through a process known as catecholase activity. The catalytic action of many dinuclear copper complexes[13−15] has been developed over the past few decades, in addition to a number of manganese(II/III) complexes.[16] Recent investigations have also shown that some dinuclear nickel(II) species can also mediate such catechol oxidation.[3,17] Further, extensive studies with copper-based model complexes have shown that structural factors[13] such as metal−metal distance, exogenous bridging ligand type, coordination geometry around the metal ion, and ligand flexibility may affect their catalytic acitivity. However, for catecholase-like activity of Ni(II) complexes, no such clear structural correlations have been drawn because the number of complexes studied for this purpose are scarce.

In this study, we have synthesized and characterized four nickel(II) complexes by using two monocondensed Schiff-base ligands, 3-[2-(diethylamino)ethylimino]butan-2-one oxime (HL^1) and 3-[3-(dimethylamino)propylimino]butan-2-one oxime (HL^2). HL^1 and HL^2 resulted in the dinuclear $[Ni_2L^1_2](ClO_4)_2$ (**1**) and trinuclear $[Ni_3(HL^2)_3(\mu_3\text{-}O)](ClO_4)_4\cdot CH_3CN$ (**2**) complexes, respectively. However, these ligands produce tetranuclear species $[\{Ni(deen)(H_2O)\}_2(\mu_3\text{-}OH)_2\{Ni_2(moda)_4\}](ClO_4)_2\cdot 2CH_3CN$ (**3**) and $[\{Ni(dmpn)(CH_3CN)\}_2(\mu_3\text{-}OH)_2\{Ni_2(moda)_4\}](ClO_4)_2\cdot CH_3CN$ (**4**) in the presence of NaOH. As **3** and **4** possess a rhombic topology, reported to be a good model for studying spin-frustration,[9,10] the magnetic properties were studied in detail. The catecholase-like activity of these four oxime-based Ni(II) complexes was examined, and it was found that only **3** and **4** act as catalysts for the areal oxidation of 3,5-di-*tert*-butylcatechol to the corresponding *o*-quinone. Unlike **1** and **2**, which display no catalytic behavior or magnetic ordering, **3** and **4** demonstrate both, making them quite interesting multifunctional materials.

EXPERIMENTAL SECTION

Starting Materials. Diacetyl monoxime (modaH), 2-(diethylamino)ethylamine (deen), 3-(dimethylamino)-1-propylamine (dmpn), and sodium hydroxide were purchased from commercial sources and used as received. Nickel perchlorate hexahydrate was prepared by the standard laboratory method; solvents were of reagent grade and used without further purification.

Caution! *Perchlorate salts of metal complexes coordinated with organic ligands are potentially explosive. Only a small amount of material should be prepared, and it should be handled with care.*

Synthesis of Schiff Base Ligands (HL^1 and HL^2). The two monocondensed Schiff base ligands, 3-[2-(diethylamino)ethylimino]-butan-2-one oxime (HL^1) and 3-[3-(dimethylamino)propylimino]-butan-2-one oxime (HL^2) were prepared by standard methods. Briefly, 8 mmol of diacetyl monoxime (0.808 g) was mixed with 8 mmol of the required amine 2-(diethylamino)ethylamine (1.080 mL)] and [3-(dimethylamino)-1-propylamine (1.008 mL) in ethanol separately (20 mL). The resulting solutions were refluxed for ca. 5 h and allowed to cool. The yellow ethanolic solutions were used directly for complex formation.

Synthesis of Complexes $[Ni_2L^1_2](ClO_4)_2$ (1) and $[Ni_3(HL^2)_3(\mu_3\text{-}O)](ClO_4)_4\cdot CH_3CN$ (2). With constant stirring, an ethanolic solution (15 mL) of $Ni(ClO_4)_2\cdot 6H_2O$ (0.728 g, 2 mmol) was added to an ethanol solution of HL^1 (2 mmol, 5 mL), resulting in the immediate precipitation of a red crystalline compound. The mixture was further stirred for 1 h at room temperature, with the amount of product gradually increasing. It was then filtered and washed with diethyl ether and redissolved in CH_3CN. Red, rectangular-shaped crystals of complex **1** suitable for single-crystal X-ray diffraction (sc-XRD) were then obtained by slow evaporation of the solvent. Complex **2** was synthesized in the same manner as **1**, except HL^2 was used instead of HL^1. High-quality crystals were obtained through slow evaporation of CH_3CN, resulting in red, rhombic-shaped crystals. Both **1** and **2** were then washed with diethyl ether and dried in a desiccator containing anhydrous $CaCl_2$ and then characterized by elemental analysis, spectroscopic methods, and X-ray diffraction.

Complex **1**. Yield: 0.580 g (82%). IR (KBr pallet, cm^{-1}): 3438mb, 2974m, 1628w, 1510m, 1449m, 1383m, 1229m, 1092sb, 744m and 619m. UV/vis: λ_{max} (nm) [ε_{max} (M^{-1} cm^{-1})] (CH_3CN) = 570 (130), 360 (630), 270 (1889) and 228 (1739). Anal. Calcd for $C_{20}H_{40}N_6O_{10}Cl_2Ni_2$: C, 33.70; H, 5.66; N, 16.47. Found: C, 33.63; H, 5.52; N, 16.31.

Complex **2**. Yield: 0.593 g (75%). IR (KBr pallet, cm^{-1}): 3459mb, 3117mb, 2940w, 1610w, 1527m, 1468m, 1383m, 1227m, 1095sb, 744m and 622m. UV/vis: λ_{max} (nm) [ε_{max} (M^{-1} cm^{-1})] (CH_3CN) = 572 (140), 328 (1069), 279 (1894) and 220 (1800). Anal. Calcd for $C_{29}H_{60}N_{10}O_{20}Cl_4Ni_3$: C, 29.35; H, 5.10; N, 14.84. Found: C, 29.43; H, 5.12; N, 14.77.

Synthesis of Complexes $[\{Ni(deen)(H_2O)\}_2(\mu_3\text{-}OH)_2\{Ni_2(moda)_4\}](ClO_4)_2\cdot 2CH_3CN$ (3) and $[\{Ni(dmpn)(CH_3CN)\}_2(\mu_3\text{-}OH)_2\{Ni_2(moda)_4\}](ClO_4)_2\cdot CH_3CN$ (4). An ethanolic solution (15 mL) of $Ni(ClO_4)_2\cdot 6H_2O$ (0.728 g, 2 mmol) was added to a mixture containing an ethanol solution of HL^1 (2 mmol, 5 mL) and NaOH (0.120 g, 3 mmol). Continual stirring of the mixture for 1 h at room temperature resulted in a green crystalline precipitate, which was filtered and washed with diethyl ether and then redissolved in CH_3CN. Green parallelepiped-shaped crystals of complex **3** suitable for XRD were obtained after the solution stood overnight in air. Similarly, single crystals of **4** were obtained by following the same procedure for **3**, but using HL^2 instead of HL^1.

Complex **3**. Yield: 0.244 g (40%). IR (KBr pallet, cm^{-1}): 3553m, 3445m, 2980w, 1605m, 1450s, 1248s, 1127s, 1098sb, 977m, 658m and 625m. UV/vis: λ_{max} (nm) [ε_{max} (M^{-1} cm^{-1})] (CH_3CN) = 590 (145), 301 (2730), and 222 (2000). Anal. Calcd for $C_{32}H_{68}N_{10}O_{20}Cl_2Ni_4$: C, 31.54; H, 5.62; N, 11.49. Found: C, 31.53; H, 5.45; N, 11.37.

Complex **4**. Yield: 0.251 g (42%). IR (KBr pallet, cm^{-1}): 3542m, 3431m, 2925w, 2884w, 1610m, 1453s, 1258s, 1094sb, 975m, 658m and 626m. UV/vis: λ_{max} (nm) [ε_{max} (M^{-1} cm^{-1})] (CH_3CN) = 596 (150), 302 (2386), and 223 (2220). Anal. Calcd for $C_{30}H_{63}N_{11}O_{18}Cl_2Ni_4$: C, 30.76; H, 5.42; N, 13.15. Found: C, 30.63; H, 5.52; N, 13.17.

Physical Measurements. Elemental analyses (C, H, and N) were performed using a Perkin-Elmer 2400 series II CHN analyzer. IR spectra in KBr pellets (4000−500 cm^{-1}) were recorded using a Perkin-Elmer RXI FT-IR spectrophotometer. Electronic spectra in methanol (1200−200 nm) and solid state (750−300 nm) were recorded in a Hitachi U-3501 spectrophotometer. Variable-temperature magnetic

dx.doi.org/10.1021/ic401020m | Inorg. Chem. XXXX, XXX, XXX−XXX

Table 1. Crystal Data and Structure Refinement of Complexes 1-4

complex	1	2	3	4
formula	$C_{20}H_{40}N_6O_{10}Cl_2\ Ni_2$	$C_{29}H_{60}N_{10}O_{20}Cl_4\ Ni_3$	$C_{32}H_{68}N_{10}O_{20}\ Cl_2Ni_4$	$C_{32}H_{63}N_{11}O_{18}\ Cl_2Ni_4$
M	712.86	1186.74	1218.62	1195.67
crystal system	monoclinic	triclinic	monoclinic	monoclinic
space group	$P2_1/c$	$P\bar{1}$	$P2_1/n$	$C2/c$
a/Å	7.475(5)	12.2018(3)	14.866(5)	22.956(5)
b/Å	21.747(5)	14.4627(4)	10.451(5)	11.086(5)
c/Å	9.689(5)	16.0305(7)	17.251(5)	21.845(5)
α/deg	90	105.075(2)	90	90
β/deg	111.622(5)	95.379(2)	96.573(5)	110.440(5)
γ/deg	90	113.578(1)	90	90
V/Å^3	1464.2(13)	2440.21(15)	2662.6(17)	5209(3)
Z	2	2	2	4
D_c/g cm^{-3}	1.617	1.615	1.520	1.521
μ/mm^{-1}	1.529	1.446	1.569	1.600
F (000)	744	1232	1272	2488
R(int)	0.021	0.052	0.049	0.168
total reflections	10945	35255	18565	17722
unique reflections	2918	9904	4998	4796
$I > 2\sigma(I)$	2518	6671	3756	3410
R1, wR2	0.0386, 0.1138	0.0654, 0.2200	0.0493, 0.1485	0.0787, 0.2153
temp (K)	293	293	293	293
GOF	1.05	1.00	1.04	0.97

Scheme 1. Formation of Complexes 1−4

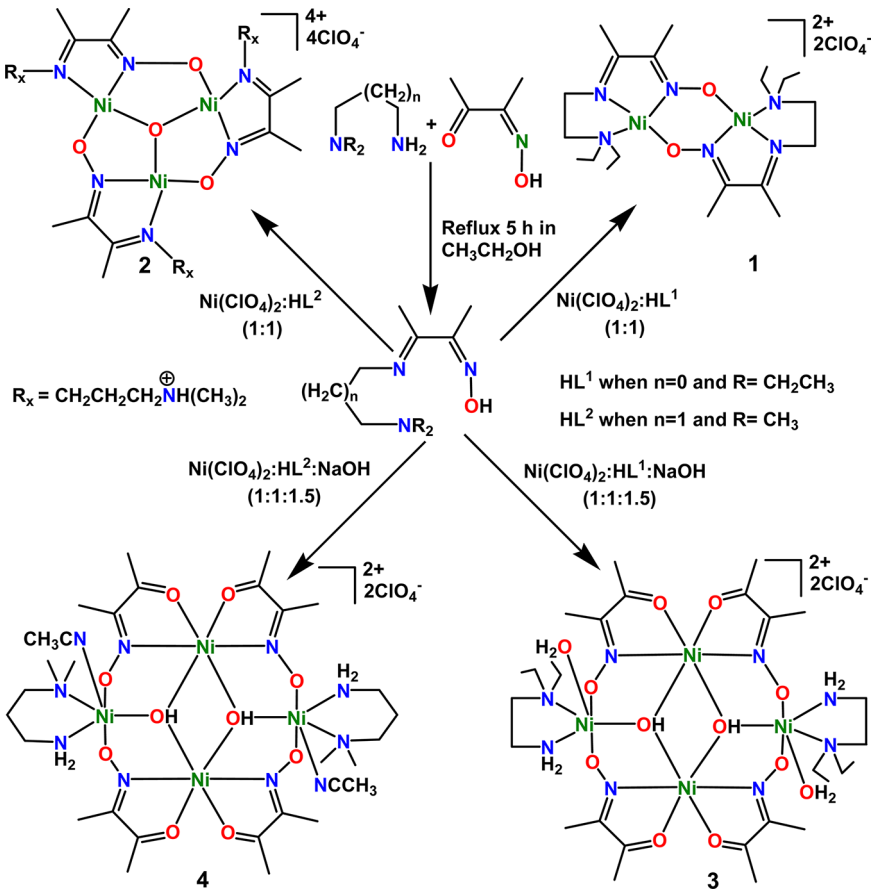

susceptibility (χ) measurements were carried out on a Quantum Design SQUID magnetometer with an applied field of 2000 G from 2 to 300 K. In order to compliment the χ data, we attempted high-frequency electron paramagnetic resonance (HF-EPR) measurements on **3** and **4** using the 375 and 240 GHz spectrometer at the National High Magnetic Field Laboratory, which have been described elsewhere.[18] In addition, X-band (9.5 GHz) EPR spectra were recorded using a JEOL JES-FA 200 instrument. Electrochemical measurements were carried out using a computer-controlled AUTOLAB (model 263A VERSASTAT) electrochemical instrument

dx.doi.org/10.1021/ic401020m | Inorg. Chem. XXXX, XXX, XXX−XXX

with Pt-tip as working electrode. Cyclic voltammograms were recorded at 25 °C versus Ag/AgCl electrode in MeCN under pure N_2 atmosphere with 0.1 M tetrabutylammonium perchlorate (TBAPC) as the supporting electrolyte. Electrospray ionization mass spectrometry (ESI-MS positive) spectra were recorded with a Micromass Qtof YA 263 mass spectrometer.

Well formed single crystals of each complex was mounted on a Bruker-AXS SMART APEX II diffractometer equipped with a graphite monochromator and Mo Kα (λ = 0.71073 Å) radiation. The crystals were positioned 60 mm from the CCD, and frames (360) were measured with a counting time of 5 s. The structures were solved using the Patterson method through the SHELXS 97 program. Non-hydrogen atoms were refined with independent anisotropic displacement parameters, while difference Fourier synthesis and least-squares refinement showed the positions of any remaining non-hydrogen atoms. The non-hydrogen atoms were refined with anisotropic thermal parameters. The hydrogen atoms bound to carbon atoms were included in geometric positions and given thermal parameters equivalent to 1.2 (or 1.5 for methyl groups) times those of the atom to which they were attached. Hydrogen atoms that bonded to N or O were located in a difference Fourier map and refined with distance constraints. Successful convergence was indicated by the maximum shift/error of 0.001 for the last cycle of the least-squares refinement. Absorption corrections were carried out using the SADABS program,[19] while all calculations were made via SHELXS 97,[20]SHELXL 97,[21] PLATON 99,[22] ORTEP-32,[23] and WINGX system ver-1.64.[24] Data collection, structure refinement parameters, and crystallographic data for the four complexes are given in Table 1.

Catalytic Oxidation of 3,5-DTBC. In order to study the catecholase activity of **1**−**4**, a 10^{-4} (M) solution of each complex (molarity was calculated taking half of the molecular weight of tetranuclear complexes **3** and **4** and two-thirds of trinuclear complex **2** to keep the same numbers of Ni(II) in solution for all four complexes and also for a comparison with dicopper system) in acetonitrile was treated with 100 equiv of 3,5-di-*tert*-butylcatechol (3,5-DTBC) dissolved in acetonitrile under aerobic conditions at room temperature. Absorbance vs wavelength (wavelength scan) of these solutions was recorded at a regular time interval of 5 min in the wavelength range 300−500 nm. To determine the dependence of rate on substrate concentration and various kinetic parameters, a 10^{-4} M solution of complexes was treated with 10, 30, 50, 70, and 100 equiv of substrate. The reactions were followed spectrophotometrically by monitoring the increase in the maximum absorbance of the quinone band at 400 nm as a function of time (time scan).

To detect the formation of hydrogen peroxide during the catalytic reaction we followed the iodometric method.[25] Reaction mixtures were prepared as in the kinetic experiments. After 1 h of reaction, the solution was acidified with H_2SO_4 until a pH of 2 was reached. In order to inhibit further oxidation, an equal volume of water was added, and the formed quinone was extracted three times with dichloromethane. To the aqueous layer, 1 mL of a 10% solution of KI and three drops of 3% solution of ammonium molybdate were added; the formation of I_3^- could be monitored spectrophotometrically due to development of the characteristic I_3^- band (λ = 353 nm, ε = 26000 M^{-1} cm^{-1}). The concentration of 3,5-DTBQ was also spectrophotometrically determined because of the development of the characteristic band at $\lambda \sim 400$ nm (ε = 26000 M^{-1} cm^{-1}).

RESULTS AND DISCUSSION

Syntheses of the Complexes. When Schiff base ligands HL^1 and HL^2 were allowed to react with nickel perchlorate hexahydrate in an EtOH medium, HL^1 resulted in the dinuclear species $[Ni_2L^1_2](ClO_4)_2$ (**1**), whereas HL^2 produced the trinuclear complex $[Ni_3(HL^2)_3(\mu_3\text{-}O)](ClO_4)_4\cdot CH_3CN$ (**2**) (Scheme 1). In both compounds, the oximato oxygen atom of Schiff base ligand is deprotonated and coordinated to Ni(II). In **1**, the tertiary nitrogen atom does not undergo protonation and instead coordinates to the metal ion. However, in **2**, the liberated proton is accepted by the same nitrogen atom of the Schiff base ligands and remains unbonded. Interestingly, when NaOH is added to deprotonate the oximato hydroxyl group, $[\{Ni(dimp)(H_2O)\}_2(\mu_3\text{-}OH)_2\{Ni_2(moda)_4\}](ClO_4)_2\cdot 2CH_3CN$ (**3**) and $[\{Ni(dimp)(CH_3CN)_2\}_2(\mu_3\text{-}OH)_2\{Ni_2(moda)_4\}](ClO_4)_2\cdot CH_3CN$ (**4**) are formed from HL^1 and HL^2, respectively (Scheme 1). In both cases, the Schiff base undergoes hydrolysis to generate the corresponding diamine and oxime molecules responsible for complex species $\{Ni(diamine)\}^{2+}$ and $\{Ni(moda)_2\}^{2+}$. Two molecules for each of these species self-assemble with the help of two hydroxyl ions, forming tetranuclear complexes **3** and **4**. It is to be noted that hydrolysis of various Schiff bases during complex formation has been observed before.[26]

IR and UV−vis Spectra. IR spectra of the complexes **1**−**4** show the characteristic bands of the coordinated oxime ligands. The bands appearing in the regions 1630−1605 and 1260−1225 cm^{-1} are due to ν(C═N) and ν(N−O) vibrational modes, respectively.[27,28] In addition, **3** and **4** display a shoulder at 3540 cm^{-1} and one broad band of medium intensity at 3450−3430 cm^{-1}. Both can be attributed to the presence of the hydroxido group, while the ν(N−H) stretching vibrations of the coordinated amino group are found in the region 3340−3300 cm^{-1}. Finally, the peaks at 1450 cm^{-1} (**3**) and 1454 cm^{-1} (**4**) are assigned to the oximate ν(C═O) vibrational modes. Moreover, all of these complexes display a couple of strong- and medium-intensity bands at ca. 1100 and 625 cm^{-1}, readily confirming the presence of ionic perchlorate.[29]

The electronic spectra of all four compounds were recorded in acetonitrile, and it was found that CT transitions dominate in all of the spectra (Figure S1, Supporting Information). Sharp, single absorption bands were found near the respective wavelengths of 360, 328, 301, and 302 nm for **1**−**4**, which can each be attributed to ligand-to-metal charge transfer transitions. In addition, a broad absorption band is observed in the visible region at 570, 572, 590, and 596 nm for **1**−**4**, respectively. This is typical for d−d transitions of Ni(II) ions with a square planar (**1** and **2**) or octahedral (**3** and **4**) environment. Moreover, an absorption band in the range 220−280 nm, assignable to intraligand charge-transfer transitions, is observed for all four complexes.

Structure Description of the Complexes. Structure **1** consists of a cationic centrosymmetric dimer $[Ni_2L^1_2]^{2+}$ [HL^1 is 3-[2-(diethylamino)ethylimino]butan-2-one oxime], together with two perchlorate anions. The cationic moiety is shown in Figure 1, while selected bond lengths and angles are summarized in Table 2. The two nickel atoms have four coordinate square planar environments bound to three nitrogen atoms of one ligand and the oximato oxygen of a second. The distances to two of the nitrogen atoms are similar, Ni(1)−N(1) 1.875(3) Å and Ni(1)−N(2) 1.833(3) Å, but shorter than that to the tertiary nitrogen Ni(1)−N(3) 1.955(3) Å. The Ni(1)−O(1)^a oxygen bond is 1.836(3) Å. Moreover, the four donor atoms show a root mean square (rms) deviation of 0.062 Å, while the metal atoms are 0.010(1) Å from the least squared planes through them. The dihedral angles between the N(imine)−Ni-N(oxime) and N(tertiary)−Ni−O are 5.86(14)°, indicating that the basal plane around the nickel atom is almost planar. This is so because the angle should be 0° for a perfectly square planar arrangement and 90° for a perfect tetrahedral arrangement. *Trans* angles around nickel [N(1)−Ni(1)−N(3) 168.77(12)° and O(1)^a−Ni(1)−N(2) 172.92(11)°] indicate slight tetrahedral distortion.

dx.doi.org/10.1021/ic401020m | *Inorg. Chem.* XXXX, XXX, XXX−XXX

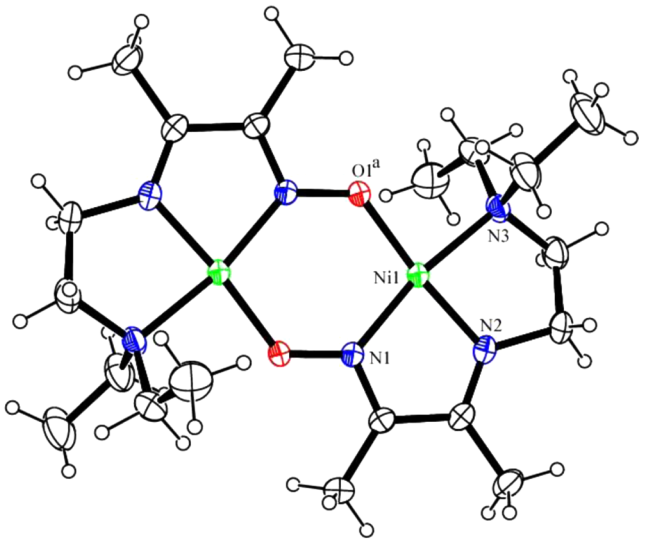

Figure 1. ORTEP view of complex **1** with ellipsoids at 30% probability. The superscript a represents symmetry code $(-x,-y,1-z)$.

Table 2. Bond Distances (Å) and Angles (deg) around Metal Atoms for Complex 1

complex **1**			
Ni(1)−N(1)	1.875(3)	N(1)−Ni(1)−N(2)	82.63(11)
Ni(1)−N(2)	1.833(3)	N(1)−Ni(1)−N(3)	168.77(12)
Ni(1)−N(3)	1.955(3)	O(1)^a-Ni(1)−N(1)	102.44(11)
Ni(1)−O(1)^a	1.836(3)	N(2)−Ni(1)−N(3)	86.57(12)
		O(1)^a-Ni(1)−N(2)	172.92(11)
		O(1)^a-Ni(1)−N(3)	88.60(12)

^{a}Symmetry element = $(-x,-y,1-z)$.

Structure **2** consists of a trinuclear cationic moiety $[Ni_3(HL^2)_3(\mu_3\text{-}O)]^{4+}$ [where HL^2 is 3-[3-(dimethylamino)-propylimino]butan-2-one oxime], four perclorate anions, and one acetonitrile molecule as a solvent. The cationic moiety is shown in Figure 2. Selected bond lengths and angles are summarized in Table 3. In the trinuclear unit, the environments of all three nickel atoms are equivalent, implying a square planar geometry. Each nickel atom is bonded to an imine nitrogen and oxime nitrogen from a ligand, another to an oximato oxygen from another ligand, and the last to a central oxido O(4) that bridges all three metal atoms. Thus, the protonated tertiary amine groups of the ligands do not coordinate the metal center and instead remain as pendant arms. These four donor atoms are approximately planar, showing rms deviations of 0.039, 0.028, and 0.013 Å with respect to the least squared planes passing through Ni(1), Ni(2), and Ni(3). The metal atoms deviate by 0.036(1), 0.044(1), 0.061(1) Å from their respective planes. Bond lengths to the μ_3-bridging oxygen atom O(4) are 1.795(5), 1.790(6), 1.797(5) Å and 1.855(4), 1.852(5), 1.858(4) Å to the oximato oxygen for Ni(1), Ni(2), and Ni(3), respectively. Distances to the nitrogen atoms range from 1.833(4)−1.895(5) Å; Ni−N (oxime) bond distances [1.838(4), 1.842(5), and 1.833(4) Å] are considerably shorter than Ni−N (imine) bond distances [1.882(5), 1.890(5), and 1.895(5) Å]. In addition, the bridging oxygen atom O(4) lies 0.113(8) Å from the plane of the three nickel atoms. The ranges of both *trans* angles [171.5(2)−177.38(18)°] and of *cis* angles [82.9(2)−94.7(2)°] are close to their respective ideal values of 180° and 90°.

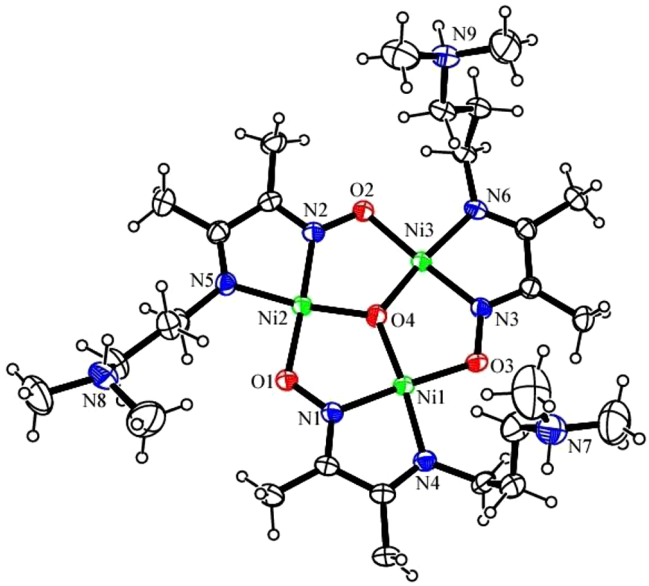

Figure 2. ORTEP view of complex **2** with ellipsoids at 30% probability. Perchlorate ions and acetonitrile molecule are not shown here.

Structure **3** consists of a cationic centrosymmetric tetranuclear unit of $[\{Ni(deen)(H_2O)\}_2(\mu_3\text{-}OH)_2\{Ni_2(moda)_4\}]^{2+}$ (where deen is 2-(diethylamino)ethylamin and modaH is butane-2,3-dione monooxime) with two perchlorate anions and two acetonitrile molecules from the solvent. Cationic moiety of **3** is shown in Figure 3, while selected bond lengths and angles are summarized in Table 4. The environment around all four nickel atoms is distorted octahedral, with the basal plane around the central Ni(1) being constituted of two oximate nitrogen atoms [N(3) and N(4)] of two different moda$^-$ anions, one ketone oxygen atom [O(3)] of moda$^-$ anions and another oxygen [O(1)^a] from a μ_3-OH$^-$ group. These four donors show a rms deviation of 0.189 Å from their mean plane, and each metal atom is displaced 0.039(1) Å from the same plane in the direction of O(1). The basal bond distances around the Ni(1) atom are in the range of 2.019(3)−2.130(3) Å, and the apical bond lengths to ketone oxygen [O(4)] of moda$^-$ anions and oxygen [O(1)] from the μ_3-OH$^-$ group are 2.120(3) and 2.037(3) Å, respectively, while the O(4)−Ni(1)−O(1) angle is 165.45(12)°. Similar to Ni(1), the coordination sphere of terminal Ni(2) has a basal plane consisting of N(1), N(2) [primary and tertiary nitrogens of amine], O(1) [from μ_3-OH$^-$ group] and O(2)^a [oximato oxygen of moda$^-$ anions], with bond distances in the range of 2.012(3)−2.194(5) Å. The apical positions are occupied by the other two oxygen atoms from the moda$^-$ anions and water solvent at Ni(2)−O(5) 2.032(3) Å and Ni(2)−O(6) 2.203(3) Å, respectively, with the bond angle O(5)−Ni(2)−O(6) being 178.93(15)°. The r.m.s. deviation of four equatorial coordinating atoms is 0.028 Å from their mean plane, and that of Ni(2) from the same plane is 0.022(1) Å in the direction of O(5) atom.

Structure **4** also consists of centrosymmetric tetranuclear units $[\{Ni(dmpn)(CH_3CN)\}_2(\mu_3\text{−}OH)_2\{Ni_2(moda)_4\}]^{2+}$ (where dmpn is 3-(dimethylamino)-1-propylamin and modaH is butane-2,3-dione monooxime), two perchlorate anions, and one acetonitrile molecule as a solvent. The cationic moiety of **4** is shown in Figure 4, while selected bond lengths and angles are

dx.doi.org/10.1021/ic401020m | *Inorg. Chem.* XXXX, XXX, XXX−XXX

Table 3. Bond Distances (Å) and Angles (deg) around Metal Atoms for Complex 2

complex 2					
Ni(1)−O(3)	1.855(4)	Ni(2)−O(1)	1.852(5)	Ni(3)−O(2)	1.858(4)
Ni(1)−O(4)	1.795(5)	Ni(2)−O(4)	1.790(6)	Ni(3)−O(4)	1.797(5)
Ni(1)−N(1)	1.838(4)	Ni(2)−N(2)	1.842(5)	Ni(3)−N(3)	1.833(4)
Ni(1)−N(4)	1.882(5)	Ni(2)−N(5)	1.890(4)	Ni(3)−N(6)	1.895(5)
O(3)−Ni(1)−O(4)	92.4(2)	O(1)−Ni(2)−O(4)	93.3(2)	O(2)−Ni(3)−O(4)	92.5(2)
O(3)−Ni(1)−N(1)	177.38(18)	O(1)−Ni(2)−N(2)	177.1(2)	O(2)−Ni(3)−N(3)	176.5(2)
O(3)−Ni(1)−N(4)	94.5(2)	O(1)−Ni(2)−N(5)	93.97(19)	O(2)−Ni(3)−N(6)	94.7(2)
O(4)−Ni(1)−N(1)	90.2(2)	O(4)−Ni(2)−N(2)	89.4(2)	O(4)−Ni(3)−N(3)	89.6(2)
O(4)−Ni(1)−N(4)	171.8(3)	O(4)−Ni(2)−N(5)	171.6(3)	O(4)−Ni(3)−N(6)	171.5(2)
N(1)−Ni(1)−N(4)	82.9(2)	N(2)−Ni(2)−N(5)	83.23(19)	N(3)−Ni(3)−N(6)	83.0(2)

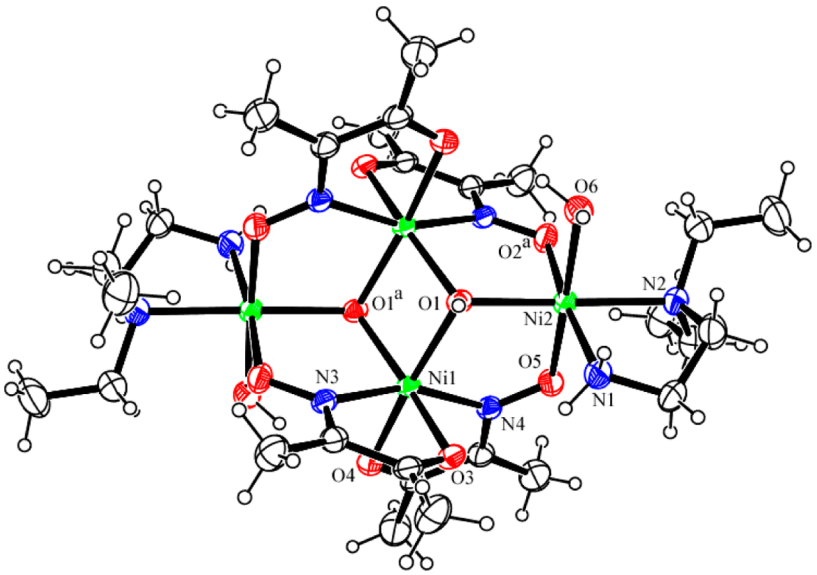

Figure 3. ORTEP view of complex 3 with ellipsoids at 30% probability. The superscript a represents symmetry code (1−x,1−y,1−z). Perchlorate ions and acetonitrile molecules are not shown here.

summarized in Table 4. The molecular structure of 4 is very similar to that of 3, with the differences being that the amine molecule is 3-(dimethylamino)-1-propylamin instead of 2-(diethylamino)ethylamin, and the coordinated solvent molecule to Ni(2) is acetonitrile instead of water. All of the donor atoms in the coordination spheres of the Ni centers are bonded in similar fashion to that of 3. Thus, the basal planes around Ni(1) centers consist of two nitrogen atoms [N(3) and N(4)] and two oxygen atoms [O(1)^b and O(4)]. The r.m.s. deviation of these four donor atoms from their mean plane is 0.154 Å. Similarly, the r.m.s. deviation of the four basal donor atoms [N(1), N(2), O(1), and O(2)] around Ni(2) from their mean planes is 0.001 Å, while Ni(1) and Ni(2) deviate from the mean plane by 0.054(1)Å and 0.024(1) Å in the direction of O(1) and N(5), respectively. The Ni−O and Ni−N distances in the basal planes are in the range 2.071(4)−2.140(5) Å and 2.051(4)−2.248(6) Å, respectively, while apical bond lengths are Ni(1)−O(1) 2.075(4) Å, Ni(1)−O(4) 2.125(4) Å, Ni(2)−O(5)^b 2.058(5) Å, and Ni(2)−N(5) 2.136(7) Å. The trans angles between the apical atoms are O(1)^b−Ni(1)−O(4) 165.42(15)° and O(5)^b−Ni(2)−N(5) 179.5(2)°. All these bond distances and angles show only minor variations from those of 3.

Complexes 3 and 4 crystallize in different monoclinic unit cells but have similar structures with very minor differences. Herein, subscripts "c" and "t" will refer to the central nickel(II) [Ni(1)] and terminal nickel(II) [Ni(2)] atoms, respectively. In both complexes, four Ni atoms form a rhomb plane within its Ni_4O_2 core. The larger structure as shown in Figure 5 is based on a rhombic "chair", with two central nickel atoms (Ni_c) having distorted octahedral N_2O_4 donor sets bridged by hydroxyl ions that form a central $Ni_{c2}O_2$ rhombus. Two terminal nickel(II) atoms (Ni_t) are bonded to μ_3-OH^- groups on each side of the rhombus such that each μ_3-OH^- group acts as a bridge among three nickel(II) atoms. The different amine ligands have no significant influence on the molecular structure of the complex cations of 3 and 4. Thus, the hydroxo bridging angles and the metal−metal distances of the central and terminal nickel atoms are very similar. Specifically, the Ni_c−O−Ni_c and Ni_c−O−Ni_t angles are 97.43(12) and 112.50(13)° for 3 and 97.11(16) and 112.37(16)° for 4. The Ni_c−Ni_c and Ni_c−Ni_t distances are 3.071(2) and 3.428(2) Å for 3 and 3.116(2) and 3.496(2) Å for 4.

A CSD search for Ni(II) complexes containing a diacetylmonoxime-based monocondensed tridentate Schiff base ligands reveals that only five Ni(II) complexes are reported. Among them, three are mononuclear,[30] one is dinuclear,[31] and one is trinuclear.[32] Therefore, complexes 1 and 2 are only the second example of dinuclear and trinuclear Ni(II) complexes, respectively. Moreover, there are some tetranuclear Ni(II) complexes possessing either rhombic[9,10,33−36] or butterfly topology,[37,38] the majority of which

dx.doi.org/10.1021/ic401020m | Inorg. Chem. XXXX, XXX, XXX−XXX

Table 4. Bond Distances (Å) and Angles (deg) around Metal Atoms for Complexes 3 and 4

	complex 3	complex 4
Ni(1)−O(1)	2.037(3)	2.075(4)
Ni(1)−O(3)	2.130(3)	2.140(5)
Ni(1)−O(4)	2.120(3)	2.125(4)
Ni(1)−N(3)	2.019(3)	2.051(4)
Ni(1)−N(4)	2.023(4)	2.061(4)
Ni(1)−O(1)^{a,b}	2.050(3)	2.082(4)
Ni(2)−O(1)	2.073(3)	2.133(4)
Ni(2)−O(2)^{a}	2.012(3)	2.071(4)
Ni(2)−N(1)	2.068(4)	2.121(6)
Ni(2)−N(2)	2.194(5)	2.248(6)
Ni(2)−O(6)/N(5)	2.203(3)	2.136(7)
Ni(2)−O(5)^{b}	2.032(3)	2.058(5)
O(1)^{a}−Ni(1)−O(3)	163.19(11)	164.85(17)
O(1)^{a}−Ni(1)−O(4)	92.39(11)	92.91(16)
O(1)^{a}−Ni(1)−N(3)	89.66(12)	90.41(16)
O(1)^{a}−Ni(1)−N(4)	106.20(12)	102.40(16)
O(1)−Ni(1)−O(1)^{a,b}	82.57(10)	82.89(15)
O(3)−Ni(1)−O(4)	97.70(12)	95.55(17)
O(3)−Ni(1)−N(3)	76.86(13)	77.25(17)
O(3)−Ni(1)−N(4)	89.22(13)	91.70(17)
O(1)^{b}−Ni(1)−O(3)	90.59(11)	91.78(16)
O(4)−Ni(1)−N(3)	90.75(13)	88.88(17)
O(4)−Ni(1)−N(4)	76.89(14)	77.42(17)
O(1)^{b}−Ni(1)−O(4)	165.45(12)	165.42(15)
N(3)−Ni(1)−N(4)	160.07(14)	161.58(18)
O(1)^{b}−Ni(1)−N(3)	102.82(12)	105.06(17)
O(1)^{b}−Ni(1)−N(4)	91.36(13)	89.79(17)
O(1)−Ni(2)−O(2)^{a}	92.30(11)	91.61(15)
O(1)−Ni(2)−N(1)	94.05(14)	90.05(19)
O(1)−Ni(2)−N(2)	176.67(12)	178.7(2)
O(1)−Ni(2)−O(6)/N(5)	85.53(13)	88.71(19)
O(1)−Ni(2)−O(5)^{b}	93.40(11)	91.83(16)
O(2)^{a}−Ni(2)−N(1)	173.66(15)	177.8(2)
O(2)^{a}−Ni(2)−N(2)	89.66(13)	87.6(2)
O(2)^{a}−Ni(2)−O(6)/N(5)	90.96(13)	94.5(2)
O(2)^{a}−Ni(2)−O(5)^{b}	89.21(13)	85.38(17)
N(1)−Ni(2)−N(2)	84.00(16)	90.8(2)
N(1)−Ni(2)−O(6)/N(5)	89.53(14)	86.9(3)
O(5)^{b}−Ni(2)−N(1)	90.42(14)	93.2(2)
N(2)−Ni(2)−O(6)/N(5)	91.74(15)	92.6(2)
O(5)^{b}−Ni(2)−N(2)	89.32(14)	87.0(2)
O(5)^{b}−Ni(2)−O(6)/N(5)	178.93(15)	179.5(2)

^{a}Symmetry element = (1−*x*,1−*y*,1−*z*) for **3**. ^{b}Symmetry element = (1/2−*x*,1/2−*y*,−*z*) for **4**.

were prepared by insertion of nickel(II) ions into polyoxotungstates,[33−35] or they contain trimethylacetates[36] or carbonate[8] as bridging groups. Pavlishchuk et al reported three rhombic tetranuclear Ni(II) complexes[9,10] containing diacetylmonooxime and different tridentate ligands (NNN, NNO and NNS donors). It may be mentioned here that all of the reported oxime containing tetranuclear complexes were obtained by mixing the required components separately at fixed molar ratios. In the present case, complexes **3** and **4** are formed by the hydrolysis of monocondensed tridentate oxime based Schiff base ligands.

Magnetostructual Properties. χ measurements on powder samples of **3** and **4** were carried out on a Quantum Design MPMS XL magnetometer from 2 to 300 K with an

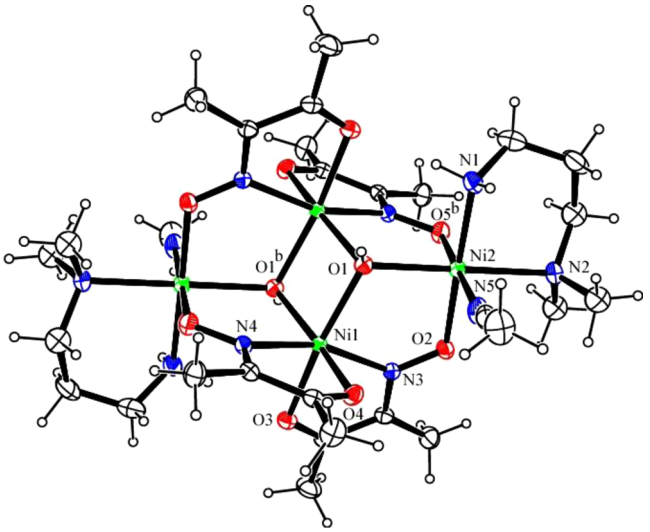

Figure 4. ORTEP view of complex **4** with ellipsoids at 30% probability. The superscript b represents symmetry code (1/2−*x*,1/2−*y*,−*z*). Perchlorate ions and acetonitrile molecule are not shown here.

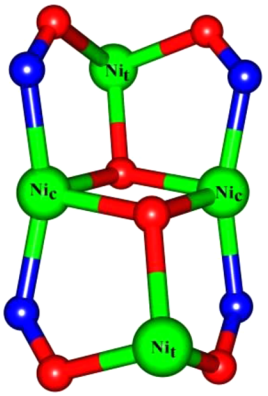

Figure 5. $Ni_4N_4O_6$ "chair" core of complexes **3** and **4** (green = Ni, blue = N, red = O).

applied field of 2000 G; **1** and **2** were neglected because of their diamagnetism. As seen in Figure 6, χT approaches zero with descending temperature for both complexes, indicating that the dominant interaction is of antiferromagnetic (AF) character;

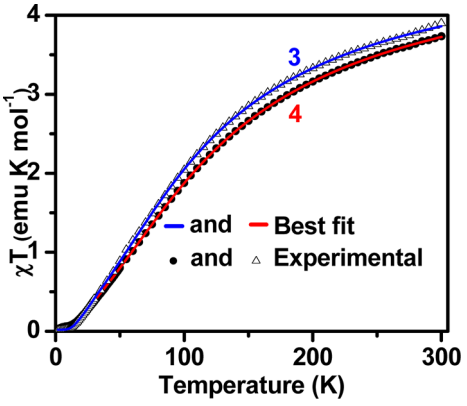

Figure 6. Plots of χT *vs* T for **3** and **4**. Points represent the experimental data, while the solid lines are representative of the corresponding best least-squares-fit according to eqs 1−3

dx.doi.org/10.1021/ic401020m | *Inorg. Chem.* XXXX, XXX, XXX−XXX

this behavior is quite common for similar compounds found in the literature.[9,10] The respective maxima of **3** and **4** are 3.90 and 3.73 emu K mol^{-1}, both of which are fairly close to the expected value of 4.0 emu K mol^{-1} for four noninteracting Ni(II) (S = 1) ions when g = 2.0. As expected, the behavior of both tetramers was not significantly different from one another given their similar ligand environments.

The spin topology of the nickel(II) core is that of a rhombus as displayed in Figure 7; the symmetry simplifies the general

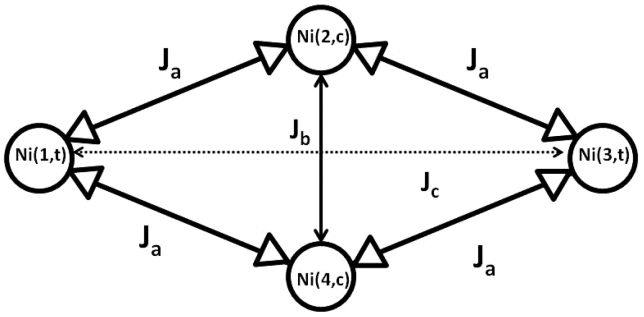

Figure 7. Magnetic coupling scheme for tetranuclear complexes **3** and **4**.

spin Hamiltonian into eq 1, which only requires three isotropic spin interactions to account for χ of the two tetramers. Interactions J_a, J_b, and J_c, respectively correspond with interactions between Ni$_c$−Ni$_t$, Ni$_c$−Ni$_c$, and Ni$_t$−Ni$_t$. The relatively large distance between the terminal ions allows one to reasonably neglect J_c, though this was verified through the fitting; the reduced χ^2 as observed in eq 2 (herein labeled as χ^2_{red}) was not improved by accounting for it.

Finding the eigenstates is further simplified by applying the Kambe coupling scheme.[39] When applying it to our problem, pairwise couplings of two spin centers are assumed, i.e., $S_{13} = S_1 + S_3$ and $S_{24} = S_2 + S_4$, with each of these states varying integrally from 0 to 2. In turn, S_{13} and S_{24} couple to form total spin S_T with integral quantum numbers from 0 to 4. The intermediate spin operators allow one to conveniently form an orthogonal basis set that diagonalizes the Hamiltonian, leading to eq 3.[40] The Van Vleck equation can then be applied to the resulting 19 energy states to be used in eq 4; all of the symbols have their standard meaning save ρ, which represents the mole fraction of paramagnetic impurity.[41] It should also be noted that phenomena such as temperature independent magnetism and axial zero field splitting were not considered as they, like J_c, do not significantly alter χ^2_{red}. In addition, one would risk overparameterization of the model, which has been discussed elsewhere.[34,35,40]

$$\hat{H} = -2J_a(S_1\cdot S_2 + S_1\cdot S_4 + S_2\cdot S_3 + S_3\cdot S_4) - 2J_b(S_2\cdot S_4) - 2J_c(S_1\cdot S_3) \quad (1)$$

$$R^2 = \frac{\sum[(\chi T)^{obs} - (\chi T)^{calc}]^2}{dof} \quad (2)$$

Where dof is degrees of freedom

$$E(S_T) = -J_a S_T(S_T + 1) - S_{13}(S_{13} + 1)(J_c - J_a) - S_{24}(S_{24} + 1)(J_b - J_a) + 4J_b + 4J_c \quad (3)$$

$$\chi = \frac{Ng^2\beta^2}{3kT}\left((1-\rho)\frac{\sum S_T(S_T+1)(2S_T+1)e^{-E(S_T)/kT}}{\sum(2S_T+1)e^{-E(S_T)/kT}} + 2\rho\right) \quad (4)$$

For **3**, g = 2.25(3), J_a = −43.5(1) cm^{-1}, J_b = 19(1) cm^{-1}, ρ = 0.016, and R^2 = 7.81E^{-5}. For **4**, the above procedure resulted in g = 2.27(4), J_a = −48.4(1) cm^{-1}, J_b = 15(1) cm^{-1}, ρ = 0.0427, and R^2 = 2.282E^{-5}. These parameters agree quite well with the literature,[8−10,42−46] which has made strong structural correlations for the Ni(II)−Ni(II) magnetic couplings mediated through an oxygen atom. Selected parameters relevant to the magnetic properties of teranuclear Ni(II) complexes with rhombic topology have been shown in Table 5. It has been found that the sign and magnitude of J is primarily dictated by the Ni−O−Ni angles; $|J|$ decreases until it disappears when the angle is somewhere between 95°and 100°.[10] This provides one explanation for the small magnitude of J_b for both tetramers, as **3** and **4**, respectively, possess a Ni$_c$−O−Ni$_c$ angle 97.6° and of 97.1°. Similarly, it has been shown that angles near 110° should result in AF intramolecular coupling. Thus, given the large Ni$_c$−O−Ni$_t$ angles of **3** and **4** (both 112.7°), one would expect J_a < 0.

It should also be noted that the value of J_b is imprecise when compared to the other parameters. This is so because χT is much more responsive to AF (J < 0) intramolecular couplings than to ferromagnetic (J > 0) ones in clusters of small

Table 5. Magnetic and Structural Parameters of Compounds 3 and 4 and of Other Known Rhombic Tetranuclear Ni(II) Complexes[a]

complex[b]	Ni$_c$···Ni$_c$	Ni$_c$···Ni$_t$	Ni$_c$−O−Ni$_c$	Ni$_c$−O−Ni$_t$	J_a	J_b	ref
[{Ni(dien)}$_2$(μ_3OH)$_2${Ni$_2$(moda)$_4$}](ClO$_4$)$_2$·H$_2$O	3.056	3.389, 3.382	97.61	113.01, 111.38	−19.8	4.8	9
[{Ni(dien)}$_2$(μ_3OH)$_2${Ni$_2$(moda)$_4$}](ClO$_4$)$_2$·2CH$_3$NO$_2$	3.073	3.398, 3.398	95.90	111.21, 111.21	−15.6	0	9
[{Ni(dien)}$_2$(μ_3OH)$_2${Ni$_2$(moda)$_4$}](ClO$_4$)$_2$·2H$_2$O· 2C$_4$H$_8$O$_2$	3.070	3.412, 3.397	97.73	112.37, 111.61	−20.0	10.0	9, 10
[{Ni(Odien)}$_2$(μ_3OH)$_2${Ni$_2$(moda)$_4$}](ClO$_4$)$_2$·0.6H$_2$O	3.072	3.384, 3.386	97.55	112.22, 111.70	−20.2	4.0	9
[{Ni(Sdien)}$_2$(μ_3OH)$_2${Ni$_2$(moda)$_4$}](ClO$_4$)$_2$ H$_2$O	3.073	3.398, 3.389	97.24	111.72, 111.17	−18.3	9.0	9
K$_{24}$[{β-Si$_2$Ni$_4$W$_{20}$O$_{72}$ (OH)$_4$(H$_2$O)}$_4$]·20H$_2$O	3.010	3.530	93.80	118.50, 126.70	−0.7	4.1	33
K$_6$Na$_4$[Ni$_4$(H$_2$O)$_2$(PW$_9$O$_{34}$)$_2$]·24H$_2$O	3.196	3.124, 3.109	95.50	93.40, 92.70	6.5	2.5	34, 35
3	3.071	3.403 3.428	97.43	112.50	−43.5	19.0	this work
4	3.116	3.496, 3.496	97.11	112.37	−48.4	15.0	this work

[a]Subscripts "c" and "t" refer to the central and terminal nickel atoms, respectively. Distances, angles, and J values are given in Å, deg, and cm^{-1}, respectively. [b]Key: dien =1,5-diamino-3-azapentane, Odien =1,5-diamino-3-oxapentane, Sdien =1,5-diamino-3-thiapentane, and modaH = butane-2,3-dione monooxime.

dx.doi.org/10.1021/ic401020m | Inorg. Chem. XXXX, XXX, XXX−XXX

nuclearity.[40] This has been observed for another Ni(II) tetramer chair of chair conformation; plots of the residual fit error $R^2(J_a,J_b)$ display "trough-like" extended minima along the J_b axis.[10] Interestingly enough, this kind of situation has arisen for a similarly shaped Fe(III) butterfly tetramer.[7a]

Observation of the energy level diagram serves as a useful guide for understanding the role of spin frustration on the magnetic susceptibility. Consider **4**; its first excited state, (1,2,2), is 96.3 cm^{-1} above the (0,2,2) ground state, while S_T = 4 is well removed from the it at 963 cm^{-1}; the remoteness of the singlet ground state (Figure 8) is a logical consequence of

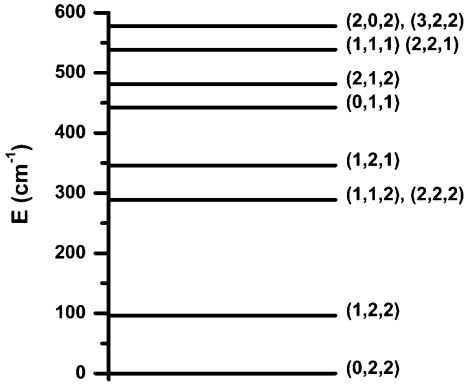

Figure 8. Energy level diagram of **4** derived from eq 3. Notation for the energy states is (S_T, S_{13}, S_{24}).

$-J_a \gg J_b$.[9] This can be seen from calculations using eq 3, which show that the energy states do not cross under this condition. But there is another important consideration to make given these circumstances. It was previously stated that **3** and **4** serve as a good model for spin frustration. Classically, this is not sensible for a singlet ground state. This makes it difficult to discern if the positive J_b is a result of direct coupling or indirectly related to other kinds. Work by Kahn has suggested that a model of competing spin interactions is more suitable.[5,46] Thus, it seems a more appropriate hypothesis to claim that J_b > 0 due to the dominating character of J_a, which in turn is driven by the larger Ni_c–Ni_t–Ni_c bond angles of the Ni(II) core; this is what dictates the alignment of Ni_c.

No signals were detected from either compound in conformity with the above analysis that predicts the ground states to be singlets. We ascribed the absence of the EPR signals to the fact that the first paramagnetic state is around 140 K above the ground state. At such high temperatures, the spin relaxation times are so short that the signals are broadened beyond detection.

The magnetic orbitals of nickel(II) with S_{Ni} = 1 are singly occupied $(d_{x2-y2})^1$ and $(d_{z2})^1$ orbitals. There are mainly three dominant interactions between nickel(II) ions and sp^2-hybridized orbitals of the NO moiety of oximato ligands:[11d] (i) antiferromagnetic coupling through the in plane bonding of Ni(II) center and NO moiety ($d_{x2-y2} \parallel \sigma_{sp2}(NO) \parallel d'_{x2-y2}$), (ii) weak antiferromagnetic coupling via in-plane bonding of the Ni(II) center and NO moiety ($d_{z2} \parallel \sigma_{sp2}(NO) \parallel d'_{z2}$), and (iii) ferromagnetic coupling by the out-of-plane bonding of the Ni(II) center and NO moiety ($d_{x2-y2} \parallel \sigma_{sp2}(NO) \perp d_{z2}$). It is important to mention that all reported oximato-bridged nickel(II) complexes exhibit overall antiferromagnetic coupling (Table 5). However, few oxime-based copper(II) complexes show weak ferromagnetic coupling via out-of plane bonding (the axial-basal bridging) between Cu(II) ions and the NO moiety.[47]

Catechol Oxidase Studies and Kinetics. 3,5-Di-*tert*-butylcatechol (3,5-DTBC) is the most widely used substrate for the study of potential catecholase activity of biomimicking coordination compounds, primarily for the following reasons: (i) its low reduction potential makes it easy to oxidize, (ii) the bulky *tert*-butyl substituents prevent further overoxidation reactions such as ring-opening,[48] and (iii) the oxidation product, 3,5-di-*tert*-butylquinone (3,5-DTBQ), is highly stable and a characteristic absorption band maxima at 402 nm (ε = 1900 $M^{-1}cm^{-1}$) in pure acetonitrile. Before the detailed kinetics studies, we first examined the catalytic activity of complexes **1**–**4** for oxidation of 3,5-di-*tert*-butylcatechol (3,5-DTBC) to *o*-quinone (3,5-DTBQ) in air-saturated acetonitrile solvent according to the reaction shown in Scheme 2.

Scheme 2. Catalytic Oxidation of 3,5-DTBC to 3,5-DTBQ in Air-Saturated Acetonitrile solvent

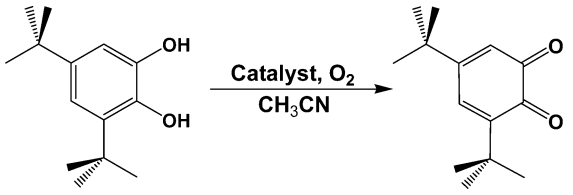

For this purpose, 10^{-4} M acetonitrile solutions of these four complexes were treated with 100 equiv of 3,5-DTBC at ambient temperature under aerobic conditions. After addition of the substrate into the complexes, the progress of the reaction was followed by recording the UV–vis spectra of the mixture at 5 min interval times. The gradual increase of an absorption band around 400 nm was observed in UV–vis spectroscopy for complexes **3** and **4**, but not for complexes **1** and **2**. This indicates that only complexes **3** and **4** catalyze the areal oxidation of 3,5-DTBC to 3,5-DTBQ. Hence, the detailed kinetic studies were only performed on complexes **3** and **4**. Figure 9 presents the variation of the spectral behavior of complex **4** in the presence of 3,5-DTBC. From Figure 9, it is clear that the spectra of **4** in acetonitrile solution shows drastic changes immediately after addition of 3,5-DTBC. Two bands

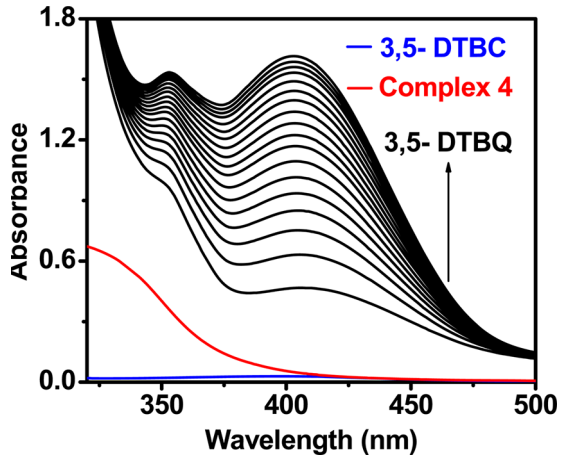

Figure 9. Increase of the quinone band at 402 nm after the addition of 100 equiv of 3,5-DTBC to an acetonitrile solution with complex **4**. The spectra were recorded at 5 min intervals.

dx.doi.org/10.1021/ic401020m | Inorg. Chem. XXXX, XXX, XXX–XXX

develop at 402 and 352 nm. It is obvious that the band at 402 nm corresponds to 3,5-DTBQ in pure acetonitrile solution. On the other hand, the band at 352 nm may indicate the formation of a stable substrate-catalyst intermediate.[16a,17b,49] The results for **1**−**3** are shown in the Supporting Information (Figures S2−S4).

The kinetics of oxidation of 3,5-DTBC to 3,5-DTBQ by **3** and **4** were determined by the method of initial rates by monitoring the growth of the quinone band at 400 nm as a function of time. The rate constant for a particular complex-substrate mixture was determined from the $\log[A_\alpha/(A_\alpha - A_t)]$ vs time plot (Figure 10). The substrate concentration

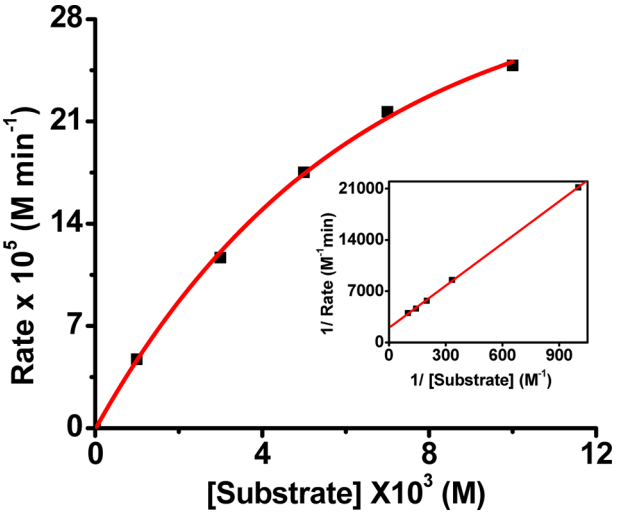

Figure 10. Plot of the rate vs substrate concentration for complex **4**. Inset shows the corresponding Lineweaver−Burk plot.

dependence of the oxidation rates and various kinetic parameters were determined by using 10^{-4} M solutions of **3** and **4** with different concentrations of 3,5-DTBC under aerobic conditions. In both cases, a first-order kinetic dependence was observed at low concentrations of 3,5-DTBC, whereas higher concentrations resulted in saturation kinetics. The observed rates versus concentration of substrate data were then analyzed on the basis of the Michaelis−Menten approach of enzymatic kinetics to get the Lineweaver−Burk (double reciprocal) plot and values of kinetic parameters V_{max}, K_M, and K_{cat}. Both the observed rate vs [substrate] and Lineweaver−Burk plot for complex **4** are shown in Figure 10. A similar plot for **3** is given in the Supporting Information (Figure S5). The kinetic parameters for both cases are listed in Table 6. The k_{cat} values can be calculated by dividing the V_{max} values by the concentration of the corresponding complexes (Table 6). This value for **4** [k_{cat} = 300.00 h^{-1}] is slightly higher than that of **3** [k_{cat} = 278.40 h^{-1}]. The k_{cat} values obtained for complexes **3** and **4** are significantly higher than those reported for dinickel(II) coordination compounds containing tridentate Schiff base ligands[3] (Table 7) and considerably lower than those reported for dinickel(II) complexes which are obtained from "end-off" compartmental Schiff base ligand.[17b,d]

Table 7. k_{cat} Values for the Oxidation of 3,5-DTBC to 3,5-DTBQ Catalyzed by Complexes 3 and 4 and Other Reported Dinuclear Ni(II) Complexes

complexes[a]	k_{cat} (h^{-1}) in CH_3CN	k_{cat} (h^{-1}) in CH_3OH	ref
$[Ni_2(L^1)_2(NCS)_2]$	64	not done	3
$[Ni_2(L^2)_2(NCS)_2]$	51	not done	3
$[Ni_2(L^3)_2(NCS)_2]$	81	not done	3
$[Ni_2(H_2L^4)(H_2O)_2(OH)(NO_3)](NO_3)_3$	inactive	14400	17b
$[Ni_2L^5(NO_3)(H_2O)_3]NO_3$	not done	1500	17d
3	278	not done	this work
4	300	not done	this work

[a]Key: HL^1 = 2- [1-(3(-methylamino)propylamino)ethyl]phenol, HL^2 = 2-[1-(2-(dimethylamino)ethylamino)ethyl]phenol, HL^3 = 2-[1-(3-(dimethylamino)propylamino)ethyl]phenol, H_2L^4 = 2,6-bis(*N*-ethyl-piperazineiminomethyl)-4-methylphenol, and H_2L^5 = *N*,*N*′-propylenebis(3-formyl-5-*tert*-butylsalicylaldimine.

To get a better understanding of the complex-substrate intermediate and a mechanistic inference of catecholase activity during the oxidation reaction, here we have recorded ESI-MS spectra of **1**, **4**, and a 1:10 mixture of the complexes to and 3,5-DTBC within 10 min of mixing in acetonitrile solvent (Figures S6−S11, Supporting Information). The spectrum of complex **1** shows a base peak at *m*/*z* = 613.17 (calcd 613.14), which can be assigned to the dinuclear species $[(Ni_2L^1_2)(ClO_4)]^+$. In addition, peaks at *m*/*z* = 256.13 and 297.28 indicate the presence of $[NiL^1]^+$ and $[(NiL^1)(CH_3CN)]^+$, respectively. On the other hand, complex **4** displays a base peak at *m*/*z* = 493.95 (calcd 494.11), which can be assigned to the cationic species $[Ni_2(dmpn)(\mu_2\text{-}OH)(moda)_2(H_2O)(CH_3CN)]^+$. The appearance of other peaks at 970.87, 868.85, 417.13, and 260.09 may be attributed to the presence of $[Ni_4(dmpn)_2(\mu_3\text{-}OH)_2(moda)_4(ClO_4)]^+$, $[Ni_4(dmpn)_2(\mu_3\text{-}OH)(\mu_3\text{-}O)(moda)_4]^+$, $[Ni_2(dmpn)(\mu_2\text{-}O)(moda)(CH_3CN)_2]^+$, and $[Ni(dmpn)(ClO_4)]^+$, respectively, for **4**. After the addition of 3,5-DTBC to the solutions of complex **1**, no changes occurred except for the appearance of a new peak at *m*/*z* = 243.18 (calcd 243.14), corresponding to the quinone sodium aggregate [3,5-DTBQ-Na]$^+$. In contrast, after the addition of 3,5-DTBC to the solutions of the complex **4**, drastic changes were observed. In addition to the quinone sodium aggregate [3,5-DTBQ-Na]$^+$ at 243.17 (calcd 243.14), the base peak at *m*/*z* = 380.28 (calcd 380.21) corresponding to $[Ni(dmpn)(3,5\text{-}DTBC^-)]^+$, and other peaks at *m*/*z* = 496.31 (calcd 496.16), 657.30 (calcd 657.23) and 1093.10 (calcd 1093.29) corresponding to $[Ni_2(dmpn)(\mu_2\text{-}OH)(3,5\text{-}DTBC^{2-})(CH_3CN)]^+$, $[Ni_2(dmpn)(\mu_2\text{-}OH)(moda)(modaH)(3,5\text{-}DTBC^-)]^+$, and $[Ni_4(dmpn)_2(\mu_3\text{-}OH)_2(moda)_4(3,5\text{-}DTBC^-)]^+$, respectively, were generated (Scheme 3). Therefore, the ESI-MS spectra allow one to conclude that the complex−substrate intermedi-

Table 6. Kinetic Parameters for the Oxidation of 3,5-DTBC Catalyzed by Complexes 3 and 4

complexes	V_{max} (M min^{-1})	std error	K_M (M)	std error	K_{cat} (h^{-1})
3	4.64×10^{-4}	1.77×10^{-5}	10.17×10^{-3}	7.8×10^{-5}	278.40
4	5.00×10^{-4}	2.50×10^{-5}	9.61×10^{-3}	1.00×10^{-4}	300.00

dx.doi.org/10.1021/ic401020m | *Inorg. Chem.* XXXX, XXX, XXX−XXX

Scheme 3. Probable Structure of Complex−Substrate Intermediates of Complex 4 According to ESI-MS Measurements

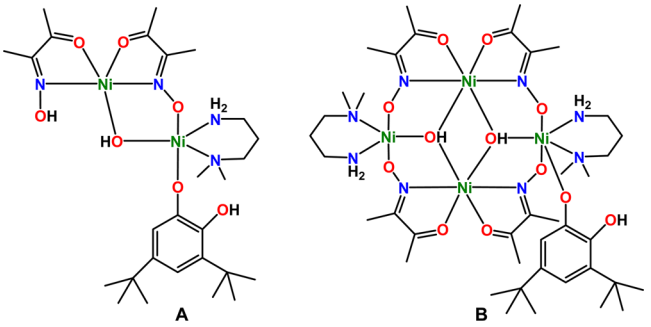

ates are formed and that seem to be responsible for the catalytic activity of the complex toward the oxidation of 3,5-DTBC to 3,5-DTBQ.

Detailed mechanistic studies with copper-based model complexes reveal that there are two possible mechanisms for the oxidation of 3,5-di-*tert*-butylcatechol to their respective quinone. One proceeds through the formation of a dicopper(II) catecholate intermediate where the dicopper(II) species stoichiometrically oxidizes the catecholic substrate to one molecule of quinone and itself reduces to a dicopper(I) species. Then, the dicopper(I) species reacts with an oxygen molecule to generate a peroxodicopper(II) adduct, which then oxidizes a second molecule of the substrate to quinone; water is formed as a byproduct through this four electron reduction process.[50] The second mechanism involves in the formation of an organic radical intermediate such as copper(I) semiquinonate.[51] Its subsequent reaction with dioxygen may result in the two-electron reduction of dioxygen, leading to the reoxidation of the copper(I) ion and release of the quinone molecule, with and hydrogen peroxide acting as a byproduct.[52]

To gain insight into the mechanism of the catalytic reaction for these Ni(II) complexes, we were interested to know whether any H_2O_2 was formed and, if so, to find its amount. The estimation of H_2O_2 clearly shows that, after approximately 1 h of oxidation, 93% and 95% H_2O_2 were generated with respect to the formation of 3,5-DTBQ for **3** and **4**, respectively. The results indicate that nearly equimolar amount of hydrogen peroxide was formed with respect to 3,5-DTBQ. Therefore, keeping analogy to the mechanism of the oxidation by using the dicopper system,[52] one might assume that the reaction proceeds through the formation of nickel(I) semiquinonate intermediate. However, this possibility seems unlikely since oximate ligands are known to stabilize higher oxidation states of nickel, i.e., Ni(III) and Ni(IV) rather than the lower one, i.e., Ni(I).[27,53] Moreover, recently Baldwin et al. reported[54] a new pathway for the aerobic substrate oxidation involving net hydrogen atom transfer from substrate to O_2 to produce hydrogen peroxide, catalyzed by an oxime based Ni(II) complex. They showed that the reaction occurred through the formation of peroxodinickel(III) adduct where dinickel(II) oximate complex was oxidized by one molecule of O_2. The subsequent reaction of this adduct with substrate molecule resulted in the oxidation of the oximate to iminoxyl radicals and reduction of Ni(III) to Ni(II) ions. Thereafter, the intermediate radical species that was produced by intramolecular hydrogen atom transfer from the coordinated substrate, which was proposed to exist either as the oxidized iminoxyl radical or the protonated neutral oxime. The catalytic cycle was completed through the consecutive release of one molecule oxidized product along with one molecule hydrogen peroxide as a byproduct.

We therefore assume that the present compounds **3** and **4** catalyzes the oxidation of catechol through similar pathways as reported by Baldwin et al.[54] We have recorded the X-band EPR spectra of the reaction mixture to understand whether any organic radical and nickel(III) complex are produced as intermediate species. For that purpose, EPR spectra of 10^{-3} M methanol solutions of each complex (**1**−**4**) added to 3,5-DTBC (10^{-1} M) were taken under aerobic conditions at room temperature at different time intervals (within 30 min) of the oxidation reaction. No signals were obtained for **1** and **2**. In contrast, an isotropic signal centered at $g_{iso} \sim 2.00$ for **3** and **4** (Figure 11 and Figure S12, Supporting Information) with a

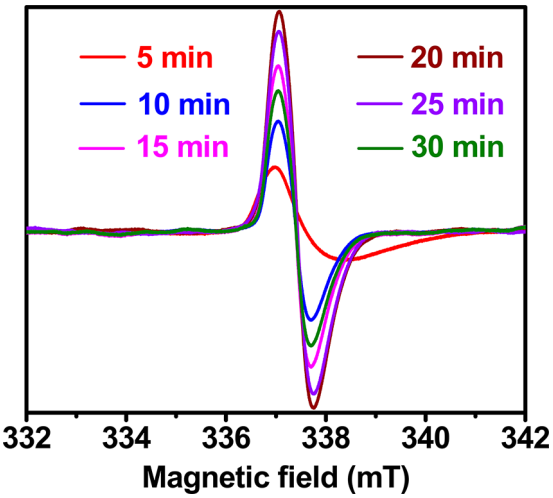

Figure 11. EPR spectrum in different time intervals of an methanol solution of complex **3** after addition of 3,5-DTBC at room temperature.

peak-to-peak line width of ca. 5−10 gauss was observed. The *g* value of the signal is close to 2.0023 (value for a free electron[55]), which is characteristic for organic radicals. The intensity of this signal gradually increases up to 20 min and then decreases. The EPR feature obtained in the present study is comparable to that observed iminoxyl radical derived from oximate group of the oxime based Ni(II) complexes.[54,56] However, we did not get any signal corresponding to the formation of the nickel(III) species as an intermediate presumably due to the its transient nature. Moreover, complexes **3** and **4** were electrochemically oxidized at room temperature in acetonitrile solution. The cyclic voltammograms showed a quasi-reversible oxidation peaks at around 0.96 and 0.88 V for **3** and **4** respectively (Figure S13, Supporting Information), which can be attributed to the Ni^{II}/Ni^{III} couple.[57]

As a reference, detailed investigations with copper-based model complexes of catechol oxidase have shown that various factors may affect their catalytic activity, such as the metal−metal distance, ligand flexibility, exogenous bridging ligand, and coordination geometry around the metal center.[13] Among the Ni(II) compounds reported herein, catecholase like activity is observed for **3** and **4**, whereas **1** and **2** are inactive toward catechol oxidation. The X-ray crystal structure makes it is clear that the coordination geometry around both terminal and

dx.doi.org/10.1021/ic401020m | *Inorg. Chem.* XXXX, XXX, XXX−XXX

central Ni(II) ions are octahedral in **3** and **4**; moreover, in both cases, the terminal nickel(II) ions are coordinated with water and acetonitrile molecules, respectively. These solvent molecules can easily be removed from Ni(II) center and create a free coordinating position for 3,5-DTBC. The coordination of 3,5-DTBC to Ni(II) is evidenced for compounds **3** and **4**. Therefore, both complexes show catecholase like activity. In contrast, the square planar geometry around Ni(II) in **1** and **2** does not permit its binding. Consequently, these are inactive toward this catalytic oxidation reaction. It was also found that **4** has slightly greater catalytic activity than **3**; it may be attributed in part to the conformational flexibility and different substitution on the nitrogen atom of the amine ligand. In the case of **4**, the longer propyl linker between the two nitrogen atoms results in a more flexible six-membered coordination ring with less hindrance between the two methyl substitutions on one of the nitrogen atoms. On the other hand, the shorter ethyl linker produces a more rigid five-membered coordination ring with more hindrance between the two ethyl substitutions on one of the nitrogen atoms in **3**. As a result, the approach and binding of the substrate to the metal center are more favorable in **4** than that of **3**.

CONCLUSIONS

In the present report, we have shown for the first time that oxime-based tridentate Schiff base ligands can be used to produce Ni(II) complexes of very different nuclearity and topology depending upon the reaction conditions and chelating ring size of the ligand moiety. HL^1, which is derived from ethylenediamine derivative, yields the dinuclear complex **1** in which metal atoms are joined only through oximato bridges. In contrast, ligand HL^2, obtained from 1,3-propanediamine derivative, produces trinuclear complex **2** containing three metal atoms in triangular arrangement through the central oxido and peripheral oximato bridges under identical reaction conditions. On the other hand, in slightly alkaline medium, both of the Schiff bases undergo hydrolysis and produce species like $\{Ni(diamine)\}^{2+}$ and $\{Ni(moda)_2\}^{2+}$, which are joined together by hydroxyl ions to form tetranuclear complexes **3** and **4**. The rhombic tetranuclear complexes consist of two different types of bridging systems between the Ni(II) ions, hydroxido and oximato. Complexes **1** and **2**, in which the geometry of Ni(II) is square planar, are found to be diamagnetic as expected, whereas **3** and **4**, having the octahedral Ni(II), show evidence of competing spin interactions. Both were found to have a singlet GS due to strong intramolecular coupling between the terminal and central nickel ions with ancillary ferromagnetic coupling between both central nickel ions. Examination of catecholase-like activity for all four complexes reveals that the ligand environment and geometry surrounding the metal play an important role for such catalytic behavior. Octahedral complexes **3** and **4** exbit catecholase like activity, but square planar species **1** and **2** are inactive. These two complexes (**3** and **4**) are the first oxime-based Ni(II) complexes whose catecholase-like activity have been investigated. Mechanistic investigations of the catalytic behaviors by X-band EPR spectroscopy and estimation of hydrogen peroxide formation indicate that the oxidation of 3,5-DTBC to 3,5-DTBC proceeds through the formation of iminoxyl-type radical. During the oxidation reaction, these oxime-based Ni(II) complexes are assumed to produce transient Ni(III) species unlike the dicopper complexes where the oxidation states of Cu(II) shuttle between +I and +II.

We are trying to develop several heterovalent as well as heteronuclear systems by using such oxime-based ligands. In particular, we aim to produce oxime-based new compounds that may show ferromagnetic behavior or increase catalytic activity by changing the metal ions, substitution of ligand system, counterions, and solvent systems.

ASSOCIATED CONTENT

Supporting Information

Spectra of obtained compounds and X-ray data (CIF). This material is available free of charge via the Internet at http://pubs.acs.org.

AUTHOR INFORMATION

Corresponding Authors

*E-mail: dalal@chem.fsu.edu.
*E-mail: ghosh_59@yahoo.com.

Notes

The authors declare no competing financial interest.

ACKNOWLEDGMENTS

L.K.D. and A.B. are thankful to CSIR, India, for awarding Senior Research Fellowships [Sanction No. 09/028 (0805)/2010-EMR-I for L.K.D. and 09/028 (0717)/2008-EMR-I for A.B.]. Crystallography was performed at the DST-FIST, India, funded Single Crystal Diffractometer Facility at the Department of Chemistry, University of Calcutta. We are grateful to Drs. Hans van Tol, Zhenxing Wang, and Andrew Ozarowski, NHMFL, for their help with EPR measurements. NHMFL is supported by the NSF Cooperative agreement No. DMR-0654118, the State of Florida, and the U.S. Department of Energy. We also thank Prof. M. G. B. Drew, School of Chemistry, The University of Reading, U.K. for the refinement of the structure of complexes **2**–**4** and Prof. R. K. Hemakumar Singh, Manipur University, India for the X-band EPR measurements. The authors also thank the Department of Science and Technology (DST), New Delhi, India, for financial support (SR/S1/IC/0034/2012).

REFERENCES

(1) (a) Qiu, S.; Zhu, G. *Coord. Chem. Rev.* **2009**, *253*, 2891–2911. (b) Decurtins, S.; Pellaux, R.; Antorrena, G.; Palacio, F. *Coord. Chem. Rev.* **1999**, *190–192*, 841–854. (c) Chelebaeva, E.; Larionova, J.; Guari, Y.; SaFerreira, R. A.; Carlos, L. D.; Paz, F. A. A.; Trifonov, A.; Guerin, C. *Inorg. Chem.* **2008**, *47*, 775–777. (d) Kitagawa, S.; Kitaura, R.; Norc, S. *Angew. Chem., Int. Ed.* **2004**, *43*, 2334–2375. (e) Forster, P. M.; Eckert, J.; Heiken, B. D.; Parise, J. B.; Yoon, J. W.; Jhung, S. H.; Chang, J.-S.; Cheetham, A. K. *J. Am. Chem. Soc.* **2006**, *128*, 16846–16850. (f) Kar, P.; Guha, P. M.; Drew, M. G. B.; Ishida, T.; Ghosh, A.; Eur, J. *Inorg. Chem.* **2011**, 2075–2085. (g) Kar, P.; Biswas, R.; Drew, M. G. B.; Ida, Y.; Ishida, T.; Ghosh, A. *Dalton Trans.* **2011**, *40*, 3295–3304. (h) Serron, S. A.; Haar, C. M.; Nolan, S. P. *Organometallics* **1997**, *16*, 5120–5123. (i) Fujita, E.; Brunschwig, B. S.; Ogata, T.; Yanagida, S. *Coord. Chem. Rev.* **1994**, *132*, 195–200. (j) Opstal, T.; Verpoort, F. *Angew. Chem., Int.Ed.* **2003**, *42*, 2876–2879. (k) Volpe, M.; Hartnett, H.; Leeland, J. W.; Wills, K.; Ogunshun, M.; Duncombe, B. J.; Wilson, C.; Blake, A. J.; McMaster, J.; Love, J. B. *Inorg. Chem.* **2009**, *48*, 5195–5207. (l) Wang, H.; Zhang, D.; Ni, Z.-H.; Li, X.; Tian, L.; Jiang, J. *Inorg. Chem.* **2009**, *48*, 5946–5956. (m) Khatua, S.; Choi, S. H.; Lee, J.; Kim, K.; Do, Y.; Churchill, D. G. *Inorg. Chem.* **2009**, *48*, 2993–2999.

(2) (a) Kar, P.; Haldar, R.; Gómez-García, C. J.; Ghosh, A. *Inorg. Chem.* **2012**, *51*, 4265–4273. (b) Biswas, A.; Das, L. K.; Drew, M. G. B.; Diaz, C.; Ghosh, A. *Inorg. Chem.* **2012**, *51*, 10111–10121.

(3) Biswas, A.; Das, L. K.; Drew, M. G. B.; Aromí, G.; Gamez, P.; Ghosh, A. *Inorg. Chem.* **2012**, *51*, 7993−8001.
(4) (a) Gatteschi, D.; Sessoli, R.; Cornia, A. *Chem. Commun.* **2000**, 725−732. (b) Gatteschi, D. *Adv. Mater.* **1994**, *6*, 635−645. (c) Biswas, R.; Ida, Y.; Baker, M. L.; Biswas, S.; Kar, P.; Nojiri, H.; Ishida, T.; Ghosh, A. *Chem.—Eur. J.* **2013**, *19*, 3943−3953.
(5) Kahn, O. *Chem. Phys. Lett.* **1997**, *265*, 109−114.
(6) (a) Zheng, Y.-Z.; Tong, M.-L.; Xue, W.; Zhang, W.-X.; Chen, X.-M.; Grandjean, F.; Long, G. J. *Angew. Chem., Int. Ed.* **2007**, *46*, 6076−6080. (b) Wills, A. S.; Harrison, A.; Ritter, C.; Simith, R. I. *Phys. Rev. B* **2000**, *61*, 6156. (c) Nocera, D. G.; Bartlett, B. M.; Grohol, D.; Papoutsakis, D.; Shores, M. P. *Chem.—Eur. J.* **2004**, *10*, 3850−3859. (d) Grohol, D.; Matan, K.; Cho, J.-H.; Lee, S.-H.; Lynn, J. W.; Nocera, D. G.; Lee, Y. S. *Nat. Mater.* **2005**, *4*, 323−328. (e) Coomer, F. C.; Harrison, A.; Oakley, G. S.; Kulda, J.; Stewart, J. R.; Stride, J. A.; Fak, B.; Taylor, J. W.; Visser, D. *J. Phys.: Condens. Matter* **2006**, *18*, 8847−8858. (f) Cave, D.; Coomer, F. C.; Molinos, E.; Klauss, H.-H.; Wood, P. T. *Angew. Chem.* **2006**, *118*, 817−820. (g) Zeng, M.-H.; Zhang, W.-X.; Chen, X.-M. *Dalton Trans.* **2006**, 5294−5303. (h) Zaworotko, M. J. *Cryst. Growth Des.* **2007**, *7*, 4−9. (i) Moulton, B.; Zaworotko, M. J. *Chem. Rev.* **2001**, *101*, 1629−1658.
(7) (a) McCusker, J. K.; Vincent, J. B.; Schmitt, E. A.; Mino, M. L.; Shin, K.; Coggin, D. K.; Hagen, P. M.; Huffman, J. C.; Christou, G.; Hendrickson, D. N. *J. Am. Chem. Soc.* **1991**, *113*, 3012−3021. (b) Vincent, J. B.; Christmas, C.; Chang, H.-R.; Li, Q.; Boyd, P. D. W.; Huffman, J. C.; Hendrickson, D. N.; Christou, G. *J. Am. Chem. Soc.* **1989**, *111*, 2086−2097.
(8) Escuer, A.; Vicente, R.; Kumara, S. B.; Mautner, F. A. *J. Chem. Soc., Dalton Trans.* **1998**, 3473−3477.
(9) Pavlishchuk, V. V.; Kolotilov, S. V.; Addison, A. W.; Prushan, M. J.; Schollmeyer, D.; Thomp- son, L. K.; Weyhermuller, T.; Goreshnik, E. A. *Dalton Trans.* **2003**, 1587−1595.
(10) Pavlishchuk, V. V.; Kolotilov, S. V.; Addison, A. W.; Prushan, M. J.; Schollmeyer, D.; Thompson, L. K.; Goreshnik, E. A. *Angew. Chem., Int. Ed.* **2001**, *40*, 4734−4737.
(11) (a) Jiang, Y.-B.; Kou, H.-Z.; Wang, R.-J.; Cui, A.-L.; Ribas, J. *Inorg. Chem.* **2005**, *44*, 709−715. (b) An, G.-Y.; Ji, C.-M.; Cui, A.-L.; Kou, H.-Z. *Inorg. Chem.* **2011**, *50*, 1079−1083. (c) Kou, H.-Z.; An, G.-Y.; Ji, C.-M.; Wang, B.-W.; Cui, A.-L. *Dalton Trans.* **2010**, *39*, 9604−9610. (d) Chaudhuri, P. *Coord. Chem. Rev.* **2003**, *243*, 143−190.
(12) Maity, D.; Mukherjee, P.; Ghosh, A.; Drew, M. G. B.; Diaz, C.; Mukhopadhyay, G. *Eur. J. Inorg. Chem.* **2010**, 807−813.
(13) Koval, I. A.; Gamez, P.; Belle, C.; Selmeczi, K.; Reedijk. *J. Chem. Soc. Rev.* **2006**, *35*, 814−840.
(14) (a) Sreenivasulu, B.; Vetrichelvan, M.; Zhao, F.; Gao, S.; Vittal, J. *J. Eur. J. Inorg. Chem.* **2005**, 4635−4645. (b) Rey, N. A.; Neves, A.; Bortoluzzi, A. J.; Pich, C. T.; Terenzi, H. *Inorg. Chem.* **2007**, *46*, 348−350.
(15) Bhardwaj, V. K.; Aliaga-Alcalde, N.; Corbella, M.; Hundal, G. *Inorg. Chim. Acta* **2010**, *363*, 97−106.
(16) (a) Banu, K. S.; Chattopadhyay, T.; Banerjee, A.; Mukherjee, M.; Bhattacharya, S.; Patra, G. K.; Zangrando, E.; Das, D. *Dalton Trans.* **2009**, 8755−8764. (b) Guha, A.; Banu, K. S.; Banerjee, A.; Ghosh, T.; Bhattacharya, S.; Zangrando, E.; Das, D. *J. Mol. Cat. A: Chem.* **2011**, *338*, 51−57. (c) Triller, M. U.; Pursche, D.; Hsieh, W.-Y.; Pecoraro, V. L.; Rompel, A.; Krebs, B. *Inorg. Chem.* **2003**, *42*, 6274−6283. (d) Majumder, A.; Goswami, S.; Batten, S. R.; Fallah, M. S. E.; Ribas, J.; Mitra, S. *Inorg. Chim. Acta* **2006**, *359*, 2375−2382.
(17) (a) Bharathi, K. S.; Sreedaran, S.; Rahiman, A. K.; Rajesh, K.; Narayanan, V. *Polyhedron* **2007**, *26*, 3993−4002. (b) Chattopadhyay, T.; Mukherjee, M.; Mondal, A.; Maiti, P.; Banerjee, A.; Banu, K. S.; Bhattacharya; Roy, S. B.; Chattopadhyay, D. J.; Mondal, T. K.; Nethaji, M.; Zangrando, E.; Das, D. *Inorg. Chem.* **2010**, *49*, 3121−3129. (c) Nirmala, G.; Rahiman, A. K.; Sreedaran, S.; Jegadeesh, R.; Raaman, N.; Narayanan, V. *J. Mol. Struct.* **2011**, *989*, 91−100. (d) Das, S.; Maiti, P.; Ghosh, T.; Zangrando, E.; Das, D. *Inorg. Chem. Commun.* **2012**, *15*, 266−268.
(18) (a) van Tol, J.; Brunel, L.-C.; Wylde, R. J. *Rev. Sci. Instrum.* **2005**, *76*, 74101. (b) Cage, B.; Hassan, A. K.; Pardi, L.; Krzystek, J.; Brunel, L.-C.; Dalal, N. S. *J. Magn. Reson.* **1997**, *124*, 495−498. (c) Bruker AXS, Inc., Madison, WI, 2002.
(19) SAINT, version 6.02; SADABS, version 2.03, Bruker AXS, Inc., Madison, WI, 2002.
(20) Sheldrick, G. M. *Program for Structure Solution*, 1997.
(21) Sheldrick, G. M. *Program for Crystal Structure Refinement*, 1997.
(22) Spek, A. L. *J. Appl. Crystallogr.* **2003**, *36*, 7−13.
(23) Farrugia, L. J. *J. Appl. Crystallogr.* **1999**, *32*, 837−838.
(24) Farrugia, L. J. *J. Appl. Crystallogr.* **1997**, *30*, 565.
(25) Neves, A.; Rossi, L. M.; Bortoluzzi, A. J.; Szpoganicz, B.; Wiezbicki, C.; Schwingel, E.; Haase, W.; Ostrovsky, S. *Inorg. Chem.* **2002**, *41*, 1788−1794.
(26) (a) Naiya, S.; Sarkar, B.; Song, Y.; Ianelli, S.; Drew, M. G. B.; Ghosh, A. *Inorg. Chim. Acta* **2010**, *363*, 2488−2495. (b) Mukherjee, P.; Drew, M. G. B.; Ghosh, A. *Eur. J. Inorg. Chem.* **2008**, 3372−3381. (c) Biswas, C.; Chattopadhyay, S.; Drew, M. G. B.; Ghosh, A. *Polyhedron* **2007**, *26*, 4411−4418.
(27) Mohanty, J. G.; Singh, R. P.; Chakravorty, A. *Inorg. Chem.* **1975**, *14*, 2178−2183.
(28) Papatriantafyllopoulou, C.; Aromi, G.; Tasiopoulos, A. J.; Nastopoulos, V.; Raptopoulou, C. P.; Teat, S. J.; Escuer, A.; Perlepes, S. P. *Eur. J. Inorg. Chem.* **2007**, 2761−2774.
(29) Nakamoto, K. *Infrared and Raman Spectra of Inorganic and Coordination Compounds*, 3rd ed.; Wiley-Interscience: New York, 1978.
(30) (a) Maity, D.; Chattopadhyay, S.; Ghosh, A.; Drew, M. G. B.; Mukhopadhyay, G. *Polyhedron* **2009**, *28*, 812−818. (b) Korvenranta, J.; Saarinen, H.; Nasakkala, E. *Finn. Chem. Lett.* **1979**, 81.
(31) Bera, M.; Noll, B. C. *Acta Crystallogr., Sect. C: Cryst. Struct. Commun.* **2007**, *63*, m553−m556.
(32) Audhya, A.; Maity, M.; Bhattacharya, K.; Clerac, R.; Chaudhury, M. *Inorg. Chem.* **2010**, *49*, 9026−9035.
(33) Kortz, U.; Jeannin, Y. P.; Hervé, G.; Isber, S. *Inorg. Chem.* **1999**, *38*, 3670−3675.
(34) Clemente-Juan, J. M.; Coronado, E.; Galán-Mascars, J. R.; Gómez-García, C. J. *Inorg.Chem.* **1999**, *38*, 55−63.
(35) Clemente-Juan, J. M.; Andres, H.; BorrÃas-Almenar, J. J.; Coronado, E.; Gadel, H. U.; Ae- bersold, M.; Kearly, G.; BÃijttner, H.; Zolliker, M. *J. Am. Chem. Soc.* **1999**, *121*, 10021−10027.
(36) (a) Sidorov, A. A.; Danilov, P. V.; Nefedov, S. E.; Golubnichnaya, M. A.; Fomina, I. G.; Ellert, O. G.; Novotvortsev, V. M.; Eremenko, I. L. *Zh. Neorg. Chim. (Russ. J. Inorg. Chem.)* **1998**, *43*, 930−938. (b) Sidorov, A. A.; Fomina, I. G.; Talismanov, S. S.; Aleksandrov, G. G.; Novotvortsev, V. M.; Nefedov, S. E.; Eremenko, I. L. *Koord. Chim. (Russ. J. Coord. Chem.)* **2001**, *27*, 584−596.
(37) Mikuriya, M.; Minowa, K.; Nagao, N. *Inorg. Chem. Commun.* **2001**, *4*, 441−443.
(38) Alexiou, M.; Dendrinou-Samara, C.; Raptopoulou, C. P.; Terzis, A.; Tangoulis, V.; Kessissoglou, D. P. *Eur. J. Inorg. Chem.* **2004**, 3822−3827.
(39) Kambe, K. *J. Phys. Soc. Jpn.* **1950**, *5*, 48−51.
(40) Sinn, E. *Coord. Chem. Rev.* **1970**, *5*, 313−347.
(41) van Vleck, J. H. *The Theory of Electric and Magnetic Susceptibilities*; Oxford University Press: Oxford, 1932.
(42) Nanda, K. K.; Thompson, L. K.; Bridson, J. N.; Nag, K. *J. Chem. Soc., Chem. Commun.* **1994**, 1337−1338.
(43) Escuer, A.; Font-Barda, M.; Kumar, S. B.; Solans, X.; Vicente, R. *Polyhedron* **1999**, *18*, 909−914.
(44) Halcrow, M. A.; Sun, J.-S.; Huffman, J. C.; Christou, G. *Inorg. Chem.* **1995**, *34*, 4167−4177.
(45) Serna, Z. E.; Lezama, L.; Urtiaga, M. K.; Arriortua, M. I.; Barandika, M. G.; Cortés, R.; Rojo, T. *Angew. Chem., Int. Ed.* **2000**, *39*, 344−347.
(46) Kahn, O. *Molecular Magnetism*; Wiley-VCH: New York, 1993.
(47) (a) Hatfield, W. E. *Inorg. Chem.* **1972**, *11*, 216−217. (b) Vaciago, A.; Zamibonelli, L. *J. Chem. Soc. Sect. A* **1970**, 218. (c) Cervera, B.; Ruiz, R.; Lloret, F.; Julve, M.; Cano, J.; Faus, J.; Bois, C.; Mrozinski, J. *J. Chem. Soc., Dalton Trans.* **1997**, 395−402.
(48) Mukherjee, J.; Mukherjee, R. *Inorg. Chim. Acta* **2002**, *337*, 429−438.

(49) Guha, A.; Chattopadhyay, T.; Paul, N. D.; Mukherjee, M.; Goswami, S.; Mondal, T. K.; Zangrando, E.; Das, D. *Inorg. Chem.* **2012**, *51*, 8750−8759.
(50) Monzani, E.; Quinti, L.; Perotti, A.; Casella, L.; Gulotti, M.; Randaccio, L.; Geremia, S.; Nardin, G.; Faleschini, P.; Tabbi, G. *Inorg. Chem.* **1998**, *37*, 553−562.
(51) (a) Mendoza-Quijano, M. R.; Ferrer-Sueta, G.; Flores-Álamo, M.; Aliaga-Alcalde, N.; Gómez-Vidales, V.; Ugalde-Saldívara, V. M.; Gasque, L. *Dalton Trans.* **2012**, *41*, 4985−4997. (b) Ackermann, J.; Meyer, F.; Kaifer, E.; Pritzkow, H. *Chem.—Eur. J.* **2002**, *8*, 247−258. (c) Kodera, M.; Kawata, T.; Kano, K.; Tachi, Y.; Itoh, S.; Kojo, S. *Bull. Chem. Soc. Jpn.* **2003**, *76*, 1957−1964. (d) Koval, I. A.; Selmeczi, K.; Belle, C.; Philouze, C.; Saint-Aman, E.; Gautier- Luneau, I.; Schuitema, A. M.; Vliet, M. v.; Gamez, P.; Roubeau, O.; Luken, M.; Krebs, B.; Lutz, M.; Spek, A. L.; Pierre, J.-L.; Reedijk, J. *Chem.—Eur. J.* **2006**, *12*, 6138−6150.
(52) (a) Peralta, R. A.; Bortoluzzi, A. J.; Szpoganicz, B.; Brandaoa, T. A. S.; Castellano, E. E.; de Oliveira, M. B.; Severino, P. C.; Terenzi, H.; Neves, A. *J. Phys. Org. Chem.* **2010**, *23*, 1000−1013. (b) Balla, J.; Kiss, T.; Jameson, R. F. *Inorg. Chem.* **1992**, *31*, 58−62. (c) Selmeczi, K.; Reglier, M.; Giorgi, M.; Speier, G. *Coord. Chem. Rev.* **2003**, *245*, 191−201.
(53) (a) Singh, A. N.; Chakravorty, A. *Inorg. Chem.* **1980**, *19*, 969−971. (b) Mandal, S.; Bose, R. N.; Reed, J. W.; Gould, E. S. *Inorg. Chem.* **1996**, *35*, 3159−3162. (c) Mandal, S.; Gould, E. S. *Inorg. Chem.* **1995**, *34*, 3993−3997. (d) Marusak, R. A.; Sharp, C.; Lappin, A. G. *Inorg. Chem.* **1990**, *29*, 4453−4456. (e) Lappin, A. G.; Martone, D. P.; Osvath, P.; Marusak, R. A. *Inorg. Chem.* **1988**, *27*, 1863−1868.
(54) Edison, S. E.; Conklin, S. D.; Kaval, N.; Cheruzel, L. E.; Krause, J. A.; Seliskar, C. J.; Heineman, W. R.; Buchanan, R. M.; Baldwin, M. J. *Inorg. Chim. Acta* **2008**, *361*, 947−955.
(55) Rieger, P. H. In *Electron Spin Resonance: Analysis and Interpretation*; Royal Society of Chemistry: Cambridge, U.K., 2007.
(56) (a) Thomas, J. R. *J. Am. Chem. Soc.* **1964**, *86*, 1446−1447. (b) Brokenshire, J. L.; Roberts, J. R.; Ingold, K. U. *J. Am. Chem. Soc.* **1972**, *94*, 7040−7049. (c) Mendenhall, G. D.; Ingold, K. U. *J. Am. Chem. Soc.* **1973**, *95*, 2963−2971.
(57) (a) Özalp-Yaman, S.; Kasumov, V. T.; Önal, A. M. *Polyhedron* **2005**, *24*, 1821−1828. (b) Yan, W.-F.; Ma, C.-Q.; Wu, J.-G.; Zhang, W.-X.; Jiang, D.-H. *Inorg. Chim. Acta* **1999**, *287*, 212−217.